



1 **Verification of Regional Deterministic Precipitation Analysis products using snow data**
2 **assimilation for application in meteorological network assessment in sparsely gauged**
3 **Nordic basins**

4 Kian Abbasnezhadi^{1,2,*†} Alain N. Rousseau¹, Étienne Foulon¹, and Stéphane Savary¹

5 1 Institut National de la Recherche Scientifique, Centre eau terre et environnement, Québec,
6 Québec, Canada

7 2 YukonU Research Centre, Yukon University, Whitehorse, Yukon, Canada

8 * Corresponding author: Climate Research Division, Science and Technology Branch,
9 Environment and Climate Change Canada, 4509 Dufferin St., Toronto, ON M3H 5T4
10 kian.abbasnezhadi@canada.ca

11 † Former address: Institut National de la Recherche Scientifique, Centre Eau Terre
12 Environnement (INRS-ETE), 490 rue de la Couronne, Québec, QC G1K 9A9, Canada.

Early Online Release: This preliminary version has been accepted for publication in *Journal of Hydrometeorology*, may be fully cited, and has been assigned DOI 10.1175/JHM-D-20-0106.1. The final typeset copyedited article will replace the EOR at the above DOI when it is published.

13 **Abstract**

14 Sparse precipitation information can result in uncertainties in hydrological modelling
15 practices. Precipitation observation network augmentation is one way to reduce the uncertainty.
16 Meanwhile, in basins with snowpack-dominated hydrology, in the absence of a high-density
17 precipitation observation network, assimilation of in situ and remotely sensed measurements of
18 snowpack state variables can also provide the possibility to reduce flow estimation uncertainty.
19 Similarly, assimilation of existing precipitation observations into gridded numerical precipitation
20 products can alleviate the adverse effects of missing information in poorly instrumented basins. In
21 Canada, the Regional Deterministic Precipitation Analysis (RDPA) data from the Canadian
22 Precipitation Analysis (CaPA) system have been increasingly applied for flow estimation in
23 sparsely gauged Nordic basins. Moreover, CaPA-RDPA data have also been applied to establish
24 observational priorities for augmenting precipitation observation networks. However, the accuracy
25 of the assimilated data should be validated before being applicable in observation network
26 assessment. The assimilation of snowpack state variables has proven to significantly improve
27 streamflow estimates, and therefore, it can provide the benchmark against which the impact of
28 assimilated precipitation data on streamflow simulation can be compared. Therefore, this study
29 introduces a parsimonious framework for performing a proxy-validation of the precipitation
30 assimilated products through the application of snow assimilation in physically-based hydrologic
31 models. This framework is demonstrated to assess the observation networks in three boreal basins
32 in Yukon, Canada. The results indicate that in most basins, the gridded analysis products generally
33 enjoyed the level of accuracy required for accurate flow simulation and therefore were applied in
34 the meteorological network assessment in those cases.

35 **1. Introduction**

36 The spatio-temporal representativeness of liquid and solid precipitation data is among the
37 most crucial factors in every flow simulation practice. Sporadic meteorological observations,
38 among other data constraints, can result in uncertainties in many hydrological modelling practices
39 performed for flow and inflow forecasting. This is also the case with the HYDROTEL system
40 (Bouda et al., 2012; Bouda et al., 2014; Fortin et al., 2001a; Turcotte et al., 2003; Turcotte et al.,
41 2007) set up for the watersheds in Yukon in northwestern Canada, where data constraints due to
42 sparsely distributed precipitation information in major basins of interest have adversely affected
43 the performance of the modelling system. Therefore, it is obvious that augmenting the precipitation
44 observation network could greatly reduce the uncertainty involved with meteorological forcing.

45 In many forecasting centers around the globe where streamflow simulation is performed in
46 basins with a hydrology dominated by snowpack melt during spring freshet, in the absence of a
47 high-density precipitation observation network, assimilation of *in situ* and remotely sensed
48 measurements of snowpack state variables has become increasingly important for accurate flow
49 estimation (Helmert et al., 2018). Li et al. (2019) have shown that in snow dominated basins, where
50 the meteorological uncertainty during the forecast period is significant (which is the case for
51 sparsely gauged networks), reinitializing the model based on observed snow water equivalent
52 (SWE) information can significantly improve streamflow forecasts. Similarly, in the absence of a
53 high-density precipitation observation network, assimilation of snowpack state variables can
54 provide the possibility to handle different sources of uncertainty by merging the value of observed
55 information into the model in order to correct the effects of model errors and improve forecasting
56 capabilities (Turcotte et al., 2010).

57 SWE reinitialization through various data assimilation (DA) approaches has been proven to
58 be an effective approach to improve the degree of agreement between the simulated and observed
59 discharge values (see, e.g., Clark et al., 2006; De Lannoy et al., 2012; Leisenring and Moradkhani,
60 2011; Nagler et al., 2008; Liu et al., 2013; Saloranta, 2016). Several DA techniques are available
61 for updating snow state variables, including direct insertion (Liston et al., 1999), Cressman
62 interpolation (Drusch et al., 2004), optimal interpolation (Brasnett, 1999), nudging (Boni et al.,
63 2010), particle filtering (Arulampalam et al., 2002), and various types of Kalman filtering
64 approaches with different levels of complexity (Gelb, 1974; Miller et al., 1994; Moradkhani, 2008;
65 Evensen, 1994). Among these approaches, Kalman filtering, and its Monte Carlo-based
66 implementation, the Ensemble Kalman Filtering (EnKF) approach, have been widely applied in
67 different hydrological modelling studies (see, e.g., Andreadis et al., 2006; Clark et al., 2006; De
68 Lannoy et al., 2012; Durand and Margulis, 2008; Huang et al., 2017; Magnusson et al., 2014;
69 Piazzini et al., 2018; Slater and Clark, 2006; Su et al., 2008).

70 Currently, to gain a proper insight into short-term, seasonal, and long-term flow forecasting
71 in northern and mid-cordilleran alpine, sub-alpine, and boreal watersheds in Yukon, where the
72 flow regime is dominated by snowpack melt, and also to alleviate the adverse effects of scarce
73 precipitation datasets, two independent DA routines are combined in HYDROTEL. These DA
74 tasks are performed to update: (i) flow states, including soil temperature, soil moisture, overland
75 flow routing, and river flow routing, based on *in situ* discharge measurements, and (ii) snow states,
76 including snow depth, SWE, snowpack thermal deficit, snowpack liquid water content, and surface
77 albedo, based on snow survey data. The first DA routine was implemented by Samuel et al. (2019),
78 where the North American Ensemble Forecasting System (NAEFS) precipitation products are
79 merged into the operational flow forecasting platform in HYDROTEL through EnKF. The snow

80 DA routine, on the other hand, performs a distributed snow correction of the simulated snowpack
81 based on available *in situ* measurements. When snow surveys are available, the simulated state
82 variables including SWE and snow depth are corrected based on site measurements. The correction
83 is performed by interpolating the three nearest sites, where measurements are taken from, over the
84 entire watershed (Turcotte et al., 2007). Thus, the application of the snow DA routine in
85 HYDROTEL is in line with the same practice followed by a number of other forecasting centers
86 (see, e.g., Brasnett, 1999; Barrett, 2003; Drusch et al., 2004).

87 There are other sources of information, such as gridded numerical products, which can reduce
88 the input data uncertainty. For instance, the numerical weather prediction datasets produced by
89 Environment and Climate Change Canada (ECCC), which are adjusted through an assimilation
90 technique known as statistical interpolation (SI), represents a prime example of such atmospheric
91 analysis gridded precipitation products. Currently, these adjusted products are created by the
92 Canadian Precipitation Analysis (CaPA) system (Fortin et al., 2015; Mahfouf et al., 2007), the
93 product of which is known as the Regional Deterministic Precipitation Analysis (RDPA). The
94 CaPA-RDPA products are currently available in grib2 format on a polar-stereographic grid with a
95 10-km resolution (true at 60°N) at two temporal resolutions (6 hourly and 24 hourly). A high-
96 resolution version of the system, known as High Resolution Deterministic Precipitation Analysis
97 (CaPA-HRDPA) System is also in operation since 2018 and takes the HRDPS 2.5-km resolution
98 field as the trial.

99 The CaPA system has gained considerable momentum in recent years, and the suitability of
100 its precipitation products for application in hydrological modelling studies in Nordic watersheds
101 in Canada have been the subject of a number of studies (e.g., Deacu et al., 2012; Eum et al., 2014;
102 Gbambie et al., 2016; Haghnegahdar et al., 2014; Hanes et al., 2016; Wong et al., 2017; Zhao,

103 2013). Boluwade et al. (2018) compared the performance of CaPA-RDPA data against
104 precipitation observations in the Lake Winnipeg basin, which entails many of the hydro-
105 climatological characteristics associated with the northern Great Plains and concluded that CaPA-
106 RDPA data is a reliable precipitation product in sparsely gauged basin. Xu et al. (2019) evaluated
107 daily total precipitation data derived from CaPA-RDPA, ERA-Interim, ERA5, JRA-55,
108 MERRA-2, and NLDAS-2 over the Assiniboine River Basin, and concluded that in general, except
109 for convective rainfalls in summer, CaPA-RDPA products demonstrated the best performance
110 among all.

111 CaPA-RDPA data have also been used for establishing observational priorities in poorly-
112 instrumented basins in Canada. For instance, Abbasnezhadi et al. (2019) used the SI technique and
113 simulated the products and by-products of the CaPA system to design a stochastic meteorological
114 network density assessment scheme. In this approach, the network assessment is undertaken with
115 the objective to maximize the accuracy of precipitation products for hydrological modelling
116 applications. This scheme can be used to find the optimal density of a new observation network,
117 only if the RDPA products in the sparsely gauged region, where the observation network is
118 investigated for augmentation, are *assumed* to represent the truth. Given such a proposition, a
119 controlled assessment approach (one in which observation uncertainty is accounted for), as
120 suggested by Abbasnezhadi et al. (2019), would then be necessary to find the optimal station
121 density. However, the benchmark that the snow assimilation routine in HYDROTEL provides for
122 accurate flow estimation would mean that the accuracy of the CaPA-RDPA products could be first
123 validated prior to undertaking the network assessment. In other words, it is possible to claim or at
124 least expect that the current SWE correction performed in HYDROTEL can result in accurate
125 streamflow estimates against which the simulated streamflow for given CaPA-RDPA forcing can

126 be compared. Such an evaluation would provide us with valuable information (i.e., benchmark)
127 with respect to the accuracy or the intrinsic added-value of using the CaPA-RDPA products in
128 sparsely gauged basins for meteorological network assessment. Given this approach, it would then
129 be possible to perform the precipitation observation network assessment through a parsimonious
130 approach. Therefore, this study was designed to provide a framework for performing a proxy-
131 validation (i.e., indirect validation of gridded weather products by means of hydrological
132 modelling) of the RDPA products through the application of snow assimilation in physically-based
133 hydrologic models. The proxy-validation experiment and the network assessment framework
134 designed in this study can therefore be undertaken to complement the precipitation network
135 assessment approach designed by Abbasnezhadi et al. (2019). The assessment scheme introduced
136 in this study may also be implemented autonomously in sparsely gauged basins; providing that
137 snow survey data would be readily available.

138 The remainder of the paper is organized as follows. In Section 2, the study area is described
139 and specific details with respect to the hydrometeorological data used in the study are provided.
140 Section 3 describes the HYDROTEL model and outlines the approaches carried out to: (a) perform
141 HYDROTEL parameter sensitivity analysis and optimization, (b) validate the CaPA-RDPA
142 products through the application of the snow data assimilation routine in the model, and (c)
143 undertake the network assessment. Thereafter, results are presented and discussed in Section 4,
144 and conclusions are drawn in Section 5.

145 **2. Study area and data characteristics**

146 **2.1 Study basins**

147 Fig. 1 illustrates the location of the three study basins in Yukon, Canada, including the Mayo
148 River basin, Aishihik (/eyzhak/) River basin, and Upper Yukon River basin. These watersheds are

149 located in northern and mid-cordilleran alpine, sub-alpine, and boreal ecoclimatic regions (Strong,
150 2013) of central and southern Yukon. The Mayo basin covers a drainage area of roughly 2,670
151 km². The mean annual precipitation and mean daily 2-m temperature are 456 mm (257 mm as rain;
152 199 mm as SWE) and -5.9°C , respectively (true for 1981-2018). The flow volume varies on a
153 seasonal basis, peaking in summer between June and July and dropping during winter in January
154 and December. There are two generating stations in Mayo: Mayo A and Mayo B. The Aishihik
155 basin covers a larger drainage area in the order of 4,550 km² and is housing the Aishihik
156 hydroelectric Facility. The mean annual precipitation is around 302 mm (126 mm as rain; 176 mm
157 as SWE), and the mean daily annual 2-m temperature is in the order of -6.6°C (true for 1981-
158 2018). The streamflow peaks in June, and the flow volume is relatively higher between May and
159 October (Brabets and Walvoord, 2009). The Upper Yukon River basin is the largest of the three
160 and covers a drainage area of around 19,600 km². The basin is mountainous and is largely covered
161 by sporadic permafrost. Runoff in the Upper Yukon is derived primarily from snowmelt and
162 rainfall. The mean annual precipitation is around 299 mm (101 mm as rain; 198 mm as SWE), and
163 the mean daily annual 2-m temperature is in the order of -3°C (true for 1981-2018). The
164 streamflow peaks in August and is low between November and May. There is a generating station
165 in Whitehorse and one control structure on Marsh Lake. For all three basins, the dominant
166 hydrological processes are governed by snow accumulation and melting that produce high flow
167 volume which peaks in summer. In addition, the Upper Yukon River summer runoff involves
168 glacier melting from the southwest region of the basin.

169 -- Fig. 1 here --

170 **2.2 Meteorological data**

171 Table 1 provides a list of the meteorological stations located within and in the vicinity of the
172 boundaries of each basin. Except for MAYOMET and AISHMET stations, which are operated by
173 Yukon Energy (YE), the other stations are operated by the Meteorological Survey of Canada
174 (MSC).

175 -- Table 1 here --

176 Fig. 2 shows the distribution of the meteorological stations within and in the vicinity of the
177 study basins. In Mayo, the precipitation gauge at the Mayo airport (Mayo A), which is located just
178 in the outskirts of the basin, is the only historical active weather station with close to 100 years of
179 available record. The MAYOMET station located near the outlet of Mayo Lake was installed in
180 late 2018 and is the only active station within the basin. In Aishihik, the majority of the stations
181 (17 out of 27) have less than 25 years of available data. There are three active MSC stations within
182 a 75-km distance from the basin boundaries, including Carmacks CS (recording since 1999),
183 Haines Junction (recording since 1944), and the one at Burwash airport, which is 50 km east of
184 Aishihik, providing more than 50 years of historical precipitation data in conjunction with its
185 nearby stations (Burwash & Burwash A). Within the basin boundaries, however, there are only
186 two weather stations available (AISHMET & Otter falls NCPC), of which Otter falls NCPC has
187 not been recording since 2015, and AISHMET is the one which was activated in late 2018. In
188 Upper Yukon, more than 65% of the stations have less than 20 years of record, the majority of
189 which have been installed in the past 10 years. The MSC station at Atlin is the only historical
190 active station with more than 120 years of recorded precipitation amounts. It should be reminded
191 that solid precipitation undercatch is rather an important issue to consider when assimilating snow
192 measurements. Pierre et al. (2019) assessed the undercatch to be as much as 20-70% of the solid

193 precipitation, which is, to the authors' knowledge, the most recent assessment available. This can
194 justify and explain why snow assimilation is necessary and beneficial.

195 -- Fig. 2 here --

196 The grib2 CaPA-RDPA v3.0.0 data from 2010 to 2018 at daily time steps were also
197 downloaded from ECCC ftp repository and decoded using NOAA/National Weather Service
198 wgrib2 program. The decoded data sets were then converted from the polar-stereographic grid onto
199 a rectangular grid covering each basin's drainage area with a spatial resolution of 0.10° in latitude
200 and 0.15° in longitude (roughly 10 km in both directions at 60°N).

201 **2.3 Hydrometric data**

202 Table 2 provides a list of available hydrometric stations at which streamflow measurements
203 are taken in each basin (see Fig. 2 for the specific location of the hydrometric stations). The inflows
204 to Aishihik Lake and Mayo Lake do not represent naturally observed discharge values and were
205 reconstructed based on recorded water levels (see Samuel et al. (2019) for a detailed description
206 of the reconstruction methodology). For Mayo Lake, water level data obtained from the 09DC005
207 station and streamflow observed at the YECMAYO station were used for reconstructing inflows.
208 Similarly, water levels recorded at station 08AA005 and streamflow recorded at 08AA008,
209 08AA009, and 08AA010 stations were used to reconstruct the inflows to Aishihik Lake. All flows
210 and water levels were provided by the Water Survey of Canada (WSC), except for those at
211 reconstructed stations #0000003, ##0000003, and YECMAYO, which are recorded by YE.

212 -- Table 2 here --

213 **2.4 Snow readings**

214 Table 3 provides the metadata of the snow depth and SWE monitoring networks managed by
215 the Water Resources Branch (WRB) of Environment Yukon as well as the Gamma Monitoring

216 (GMON) automatic snowpack sensor readings provided by YE. The GMON (a.k.a. Campbell
217 Scientific CS725) sensor measures SWE by detecting the attenuation of naturally occurring
218 electromagnetic energy from the ground. This contactless approach can offer highly reliable and
219 accurate local SWE measurements with an uncertainty level that does not exceed $\pm 5\%$ at maximum
220 snow depth. Traditional SWE measurement approaches, such as the application of snow pillows,
221 by which the snowpack weight is directly measured, are prone to higher uncertainty levels since
222 snowpack properties (e.g., radiation characteristics) can be altered during the measurement. The
223 GMON gauge, which monitors snowpack properties in a contactless mode, does not suffer from
224 the same disadvantages. During the past few years, a number of GMON gauges were installed at
225 those locations identified in Table 3 and Fig. 2 (five stations were initially installed in Upper
226 Yukon, but two were removed and relocated; one in Mayo; and one in Aishihik). Once monitored,
227 the collected information is transmitted via satellite connection and goes through quality control.
228 Added and relocated GMON gauges intend to complete the existing snow survey site or at least
229 offer specific measurements within the basin limit (in Aishihik, Mayo). *In situ* snow measurements
230 are relevant and aim to capture snow evolution, but local measurements may not be representative
231 for the entire basin conditions.

232 -- Table 3 here --

233 **3. Models and methodology**

234 **3.1 HYDROTEL: Sensitivity analysis and model calibration**

235 The semi-distributed physically based HYDROTEL model can simulate a variety of
236 hydrological processes. These processes and the physically-based approaches used to simulate
237 each one along with a list of parameters associated with each process used in the version of
238 HYDROTEL utilized in this study are listed in Table 4. In HYDROTEL, the vertical water budget

239 is computed over a computational unit called the Relatively Homogeneous Hydrological Unit
240 (RHHU), which represents either a hillslope or elementary sub-watershed and are derived based
241 on a digital elevation model and a digital network of lakes and river sections using PHYSITEL, a
242 specialized GIS for distributed hydrological models (Turcotte et al., 2001; Rousseau et al., 2011;
243 Noël et al., 2014), both of which overlaid by a multi-layer soil model. The soil column of a RHHU
244 is stratified into three layers. The first soil layer (Z1) governs infiltration, and the other two layers
245 (Z2 and Z3) control interflow and baseflow. The interpolation of meteorological variables is based
246 on the weighted mean of the nearest three stations to resolve the amount of total precipitation,
247 which is then partitioned into rain and snow according to a threshold temperature and a simple
248 weighted scheme based on daily minimum and maximum temperatures, on each RHHU. For
249 missing station values, HYDROTEL fills the gap by using the values available at the three nearest
250 stations based on the inter-station temperature and precipitation altitude variations. The
251 accumulation and melt of snowpack processes are based on a mixed degree-day energy budget
252 approach and determine the timing and peak of the spring freshet. In the glacier module, a mixed
253 degree-day energy budget approach is also used in the exact same fashion used for the snowmelt
254 process. In the soil temperature and soil frost process, the only associated parameter (soil freezing
255 temperature threshold) is not distributed over the entire RHHUs, and therefore, is not
256 recommended to be modified. The next process is designed to identify the potential
257 evapotranspiration which is dominantly going to impact the total annual runoff and baseflow in
258 summer. The flow process at the RHHU scale simulates the water flux towards the river network
259 using a hydrogeomorphological unit hydrograph (a.k.a., HGM).

260 -- Table 4 here --

261 While other studies have performed different types of sensitivity analyses of HYDROTEL on
262 other basins (e.g., Bouda et al., 2013; Turcotte et al., 2003), a global sensitivity analysis was
263 performed using the Variogram Analysis of Response Surfaces (VARS) toolbox (Razavi et al.,
264 2019). The toolbox allows the user to identify the parameters by the importance level (i.e., model
265 sensitivity to changing parameter conditions) through a multi-method approach that unifies
266 different theories and strategies. With sensitive parameters in hand, the model calibration becomes
267 a less challenging task. However, since calibration of HYDROTEL, in essence, is a multi-objective
268 optimization problem (due to the number of stream gauges reporting flows in the basin for which
269 several error criteria might be assessed), defining what makes the model calibrated is not a
270 straightforward task. Moreover, other factors affecting the quality of the calibration result include
271 error due to lake/reservoir inflow reconstruction and the quality of precipitation or temperature
272 forcing data (elaborating on these concerns is beyond the scope of the current study). To properly
273 respond to these challenges, model calibration was completed in OSTRICH (Optimization
274 Software Toolkit for Research Involving Computational Heuristics), which is a model-
275 independent and multi-algorithm optimization tool (Matott, 2017). The toolkit, which supports
276 both single- and multi-criteria optimization options, can be used for the weighted non-linear least-
277 squares calibration of the model parameters or for constrained optimization of a set of design
278 variables according to pre-defined cost functions. OSTRICH can incorporate different algorithms
279 to search for the optimal value of the objective functions and to identify the set of parameter values
280 associated with such optima. There are several optimization algorithms available in the toolkit,
281 which can be classified as either deterministic local or heuristic global search methods
282 incorporating elements of structured randomness. For multi-criteria optimization, the Pareto
283 Archive Dynamically Dimensioned Search (PA-DDS; Asadzadeh and Tolson, 2009, 2013) and the

284 simple multi-objective optimization heuristic algorithms are available, while for uncertainty-based
285 calibration, several sampling-based algorithms (i.e., Generalized Likelihood Uncertainty
286 Estimation and Metropolis-Hastings Markov Chain Monte Carlo) are available. In addition, the
287 asynchronous parallel processing architecture provided by OSTRICH, which is based on the
288 industry standard Message Passing Interface (MPI), provided the means to speed up the calibration
289 procedure.

290 The model was calibrated for the period of 2010-2018 using PA-DDS by maximizing the
291 Kling-Gupta Efficiency (KGE; Gupta et al., 2009) and minimizing the root mean squared errors
292 (RMSE). HYDROTEL was forced with CaPA-RDPA and meteorological data, including daily
293 precipitation and maximum and minimum temperatures time series described in Table 1, as well
294 as snow survey observations provided in Table 3. Daily historical discharge data measured at the
295 location of available hydrometric stations described in Table 2 and identified in Fig. 2 were
296 obtained from WSC, while the reconstructed inflows were calculated and used for model
297 calibration.

298 **3.2 Impact of snow data assimilation and CaPA-RDPA forcing**

299 In order to investigate the impact of SWE assimilation on model performance, and also to
300 understand how robust the accuracy of CaPA-RDPA products were over the three study basins for
301 hydrologic application purposes, two separate sets of modelling experiments were designed. In the
302 first set (experiment Set 1), the model was trained with forcing CaPA-RDPA, while in the second
303 set (experiment Set 2), MSC meteorological data were used as input. Depending on whether the
304 GMON and snow survey monitoring information were assimilated during the calibration and the
305 ‘stand-alone’ run (i.e., when the model runs once the calibration is completed), two separate runs
306 were considered for each set (see Table 5). In Exp. 1.1, the model was calibrated while assimilating

307 SWE measurements. The assimilation was then switched off and the calibrated model was forced
308 with CaPA-RDPA once again for the same time period (2010-2018) (Exp. 1.2). This experiment
309 was designed to indicate the extent by which the model would be able to preserve the flow
310 estimation accuracy with forcing precipitation analysis products only. The second set of
311 experiments (Exp. 2.1 and Exp. 2.2) are similar to those in the first set except that CaPA-RDPA
312 data were replaced with gauged meteorological forcing. For each experiment, goodness-of-fit
313 metrics can be used to quantitatively measure the representativeness of the experimental flow
314 estimations to the hydrometric observations (the metrics used in this study can be found in the
315 supplementary materials provided in the online version of this paper). Such an evaluation helped
316 us perform an inter-comparison of the results between the two sets of experiments.

317 -- Table 5 here --

318 **3.3 Network assessment**

319 Depending on whether the former assessment of the CaPA-RDPA forcing in HYDROTEL
320 may suggest if the gridded analysis products can be adequately used for streamflow simulation, a
321 simple network density sensitivity analysis based on CaPA gridded products was proposed for
322 flow simulation in HYDROTEL. Such an assessment was designed to guide future network
323 assessment procedures. Therefore, a network assessment procedure similar to that of
324 Abbasnezhadi et al. (2019) was followed here, except that the assessment did not include
325 artificially generated reference fields. Rather, a subset of grid points was extracted to create
326 network scenarios of different resolutions from the RDPA domain over each basin, while the
327 respective precipitation analysis was directly used during the assessment. Such an uncontrolled
328 framework could be specifically useful for the case of this study as the SWE DA-CaPA coupling
329 could prove to output such streamflow estimation that could closely match flow observations.

330 Sampling grids (Θ^v), where v is the resolution of the pseudo-network in decimal arc-degrees,
331 pertaining to each study basin are defined in Table 6 (refer to the supplementary materials to see
332 individual scenarios for each basin).

333 -- Table 6 here --

334 **4. Results and Discussion**

335 **4.1 Sensitivity analysis and model calibration**

336 The results of the sensitivity analysis provided by VARS indicated that among the parameters
337 used to regulate the vertical water budget, the second soil layer thickness ($Z2$), which affects flow
338 peaks, is a sensitive parameter. The third soil layer thickness ($Z3$), which mostly affects baseflow,
339 was identified to be a less sensitive parameter in this group. Also, the recession coefficient (CR),
340 which affects summer baseflow and works with $Z3$, was found to be a relatively sensitive
341 parameter. Among the parameters used for calculating the weighted mean of the nearest three
342 stations, VARS indicated that the third parameter in this group (PPN) has more impact on the
343 results, and the first two (GT and GP) are almost equal in sensitivity. Also, for the snow processes,
344 the melting temperature thresholds and rates for all three land classes in this group (SFC , SFF ,
345 SFD , TFC , TFF , TFD) were shown to have equal sensitivity levels. Both glacier melting
346 parameters (MR and TT) were found to be sensitive too, and the multiplicative coefficient ($FETP$)
347 applied to the Penman-Monteith equation was found to be the only sensitive evapotranspiration
348 parameter. None of the parameters related to the flow process at the RHHU scale was found to be
349 sensitive, while any modification to these parameters would force the model to recalculate the
350 HGM file which would be time-consuming. The parameters associated with the channel flow
351 process, computed using the kinematic wave equation, were also not found to be sensitive.

352 Previous VARS applications performed by Foulon et al. (2019) in two basins in southern
353 Québec yielded different results for the vertical water budget parameters. Z1 was shown to be the
354 least sensitive soil layer thickness, while Z2 and Z3 were the second most and the most sensitive
355 parameters, respectively. Also, the recession coefficient (CR) was indicated to be one of the most
356 sensitive parameters in the model. This signifies that HYDROTEL is rather sensitive to basin
357 location and governing hydrological processes. In fact, Yukon and southern Québec are both
358 governed by snow accumulation and melt, yet summer baseflow plays a more prominent role in
359 southern Québec.

360 With sensitive parameters in hand, comprising of a set of 16 parameters indicated in Table 4
361 by those with the importance level of 1, the model was calibrated in OSTRICH. The standard upper
362 and lower bound values used for each parameter in OSTRICH are provided in Table 4, which are
363 based on the physical meaning of each parameter and the works of Fortin et al. (2001b) and
364 Turcotte et al. (2003). Also, the initial estimates for each parameter were based on those derived
365 in previous calibration efforts, in which each parameter was manually adjusted in order to achieve
366 the desired hydrological performance. The toolbox utilized eight computational cores for
367 asynchronous parallel processing at the budget of 2-18 hours (depending on the basin's drainage
368 area) for 1000 iterations.

369 In Mayo, the model calibration was completed in OSTRICH based on the inflow time-series
370 into Mayo Lake associated to YE gauge ##0000003 (see Fig. 2). In Aishihik, the model calibration
371 was completed in two stages. In the first stage, the model was calibrated for Sekulmun River
372 streamflow time-series at the outlet of Sekulmun Lake observed at WSC Gauge 08AA008 (see
373 Fig. 2). The Sekulmun portion of the Aishihik model was isolated and separated in HYDROTEL
374 GUI (graphical user interface) to decrease the model run time. In the second stage, the model was

375 setup to simulate the reconstructed inflow time series to Aishihik Lake associated with YE gauge
376 #0000003. The original reconstructed inflow data display high-intensity fluctuations and were not
377 deemed suitable for the calibration. Instead, they were first smoothed by using a 7-day moving
378 average window (windows of longer durations were also tested and did not show to enhance the
379 calibration results). In Upper Yukon, the model calibration was also performed in two stages. In
380 the first stage, the model was calibrated separately for three gauged sub-basins, including Atlin
381 River (WSC gauge 09AA006), Tutshi River (WSC gauge 09AA013), and Wheaton River (WSC
382 gauge 09AA012) (see Fig. 2). In the second stage, the model was then setup to simulate the flow
383 time series in Yukon River at Whitehorse observed at WSC gauge 09AB001.

384 Fig. 3 shows the flow duration curves for Mayo, Aishihik (including the Sekulmun sub-basin),
385 and Upper Yukon (including the Atlin, Tutshi, and Wheaton sub-basins) (refer to the
386 supplementary materials provided in the online version of this paper to see discharge time-series).
387 In Mayo, the simulation has fully preserved the exceedance probability of observed flows. In
388 Aishihik and Sekulmun, other than some overestimation of winter low flows, the remainder has
389 been well captured by the model. In Upper Yukon, in general, the exceedance probabilities of the
390 simulated flows closely resemble the observed ones although the low flows are underestimated in
391 sub-basins with small drainage areas (Tutshi and Wheaton), which has similarly impacted the low
392 flows in Yukon too. In Atlin, the exceedance probability of the observed high flows (corresponding
393 to the flow peaks) is marginally underestimated.

394 -- Fig. 3 here --

395 **4.2 Proxy validation of CaPA-RDPA**

396 The impact of the snow DA routine in HYDROTEL and CaPA-RDPA forcing data on
397 modelling results were assessed based on the set of experiments discussed in Section 3.2. Fig. 4

398 compares the metrics in Mayo for the first and the second sets of experiments (for the full
399 description of the metrics used in the figures of this section, see the supplementary materials in the
400 online version of this paper). The metrics reported by the experiments indicate that the calibration
401 results for the case when CaPA-RDPA are used as input (Exp. 1.1 and Exp. 1.2) surpass, in both
402 cases, those derived by station observations (Exp. 2.1 and Exp. 2.2). In addition, the best outcome
403 is obtained with Exp. 1.1 when the model calibration is performed with CaPA-RDPA forcing and
404 the snow DA routine in active mode. Exp. 1.2 (CaPA-RDPA forcing and no snow DA), on the
405 other hand, indicates that the model's performance is not undermined if the snow DA routine is
406 turned off in HYDROTEL (when the model has already been calibrated with the snow DA routine
407 in active mode). In other words, for this experiment, the assimilation of snow monitoring data has
408 relatively no impact on the flow estimation accuracy if CaPA-RDPA data are used as input. In
409 contrast, the metrics obtained from the second set of experiments indicate that when the model is
410 calibrated using MSC meteorological data as input and with the snow DA routine in active mode
411 (Exp. 2.1), the metrics are on the ballpark of an acceptable level, while still falling short of those
412 obtained with CaPA-RDPA. However, as Exp. 2.2 indicates, if the snow DA routine is turned off,
413 the flow estimation accuracy declines significantly. This illustrates that for the second set of
414 experiments with sparsely gauged meteorological input data, the snow DA routine has a
415 compensating impact on the flow estimation accuracy.

416 Although the new GMON stations do not provide a long record of measurements yet, the snow
417 course sites in all three basins provide long-enough and continuous records of snow depth and
418 SWE measurements. Results from the second set of experiments shown in Fig. 4 indicate that, in
419 Mayo, these snow course measurements provide valuable information by which the SWE data
420 simulated using the meteorological network can be corrected through the snow assimilation routine

421 in HYDROTEL. In other words, the flow estimation accuracy in Mayo is highly dependent on the
422 external information from the snow survey sites. Although this outcome does not indicate the
423 representativeness of the snow survey sites, it hints at their value. The same debate is found in the
424 literature where hydrological models, for example, are run by interpolating snow depth
425 measurements from a few selected sites to larger areas despite their limited spatial
426 representativeness (Grünwald and Lehning, 2015; López-Moreno et al., 2013). Other studies have
427 quantified the issue of snow sites representativeness. For example, Winstral and Marks (2014)
428 proved that an index site representative of the basin conditions can be valid for a basin wide SWE
429 in most years.

430 On the other hand, the proxy validation of the CaPA-RDPA in Mayo based on the
431 reconstructed inflow associated with gauge ##0000003 shows that the analysis is accurate enough
432 to the extent that would not call for any correction through snow measurements. To this point,
433 these results indicate that in Mayo: (a) CaPA-RDPA products can be used for flow estimation, (b)
434 given the fact that very few precipitation stations are currently assimilated in CaPA, if the current
435 network is extended, the modelling accuracy will improve, and (c) in the absence of a precipitation
436 observation network with an optimal density, the snow assimilation routine plays a significant role
437 to compensate for proper precipitation information.

438 -- Fig. 4 here --

439 Fig. 5a compares the metrics in Aishihik for the first and the second sets of experiments, while
440 the performance of the model in response to the set of experiments completed in Sekulmun are
441 shown in Fig. 5b. The results reported for both Aishihik and Sekulmun are not identical to those
442 of Mayo and the experiments rather exhibit a contrasting outcome. While in Mayo, deactivating
443 the snow assimilation routine in HYDROTEL when forcing the model with CaPA-RDPA

444 (Exp. 1.2) would marginally impact the metrics compared to the case when the snow assimilation
445 routine was active (Exp. 1.1), in Aishihik (including the Sekulmun sub-basin), deactivating the
446 snow assimilation routine led the model performance to decay significantly. This suggests that the
447 RDPA gridded products do not encompass the required accuracy over Aishihik, rendering the
448 assimilation of snow readings an essential component for accurate flow estimation. The
449 inadequacy of the RDPA estimates over Aishihik is an indication of the detrimental impact of the
450 sparse precipitation network in Aishihik, which encompass a relatively larger drainage area, on
451 CaPA products over the basin. In Sekulmun, Exp. 2.2 provides marginally better results than Exp.
452 2.1, demonstrating that the precipitation measurements taken at the MSC meteorological stations
453 better represent the ground SWE accumulation than those recorded at the snow course sites.
454 Nevertheless, in Sekulmun, when using CaPA-RDPA data as the input, the combined effect of
455 incorporating the value of information from both the external assimilation of precipitation data in
456 CaPA and the internal assimilation of snow readings in HYDROTEL has obviously improved the
457 flow estimation accuracy (see Fig. 5b). In Aishihik, however, Exp. 2.1 displays a declined
458 performance relative to Exp. 1.1, while Exp. 2.1 and Exp. 2.2 are relatively identical. These results,
459 in total, revealed that in Aishihik and Sekulmun, the snow data are essential for accurate flow
460 estimation if the model is forced with CaPA-RDPA, while the MSC precipitation input data seems
461 to deliver sufficient accuracy (indicating the accuracy of the precipitation measurements taken as
462 MSC stations which necessitates minimal correction by the data taken at the snow course sites).
463 This, once again, indicates that the value of precipitation information from the MSC precipitation
464 gauges is superior to those of CaPA-RDPA which illustrates the low accuracy of CaPA data over
465 the basin.

466 -- Fig. 5 here --

467 Fig. 6 compares the metrics in Upper Yukon, including those for Atlin, Tutshi, and Wheaton
468 for the first and the second sets of experiments. In Atlin (Fig. 6a), there are marginal differences
469 between the results derived from all four experiments. This agreement could be the outcome of
470 several factors, including: (a) co-location of the snow course site and the MSC gauge in Atlin, (b)
471 existence of a MSC gauge which is assimilated in CaPA (see Fig. 2); forcing the respective RDPA
472 over the basin to become more or less identical to that of gauge reading, (c) the impact of the
473 nearby MSC gauges on the northeast side of the basin (just beyond the basin boundary) on the
474 accuracy of precipitation estimate over the basin. In Tutshi and Wheaton, however, a different
475 outcome is evident. The impact of drainage area on the flow estimation accuracy for the given
476 activity state of the snow assimilation routine seems to be a factor of importance. For instance, for
477 a sub-basin such as Tutshi (Fig. 6b) with a small drainage area, the impact of the only snow course
478 site in the basin (site #09AA-SC3) on the flow accuracy can be comprehended by the fact that
479 deactivating the snow assimilation in Exp. 2.2 has significantly decayed the flow accuracy by
480 almost half. On the other hand, in Wheaton (Fig. 6c), a sub-basin with a comparable drainage area
481 to that of Tutshi, in the absence of any snow course site, Exp. 2.2 has apparently yielded about the
482 same metrics obtained from Exp. 2.1. In general, the results of the experiments performed in Upper
483 Yukon indicate that since the basin generally enjoys a higher number of weather stations (including
484 those assimilated in CaPA and snow course sites), the results demonstrate better metric values.

485 -- Fig. 6 here --

486 Table 7 summarizes the significance of the snow assimilation routine for each basin for the
487 given meteorological forcing. In short, activating the snow assimilation routine would have a
488 significant impact on the flow estimation only in Mayo when forcing HYDROTEL with the MSC
489 meteorology and in Aishihik when forcing the model with CaPA-RDPA data. Hence, it appears

490 that snow survey sites are more representative of the watershed snow conditions than the
491 meteorological conditions recorded at the MSC stations or embedded into CaPA-RDPA.

492 In Upper Yukon, sub-basins did not yield consistent results. It was shown that the model does
493 not necessarily need the assimilation of snow products when the model is forced with either gauged
494 or analysis precipitation products (for 3 out of 4 sub regions). While medium-size watersheds (as
495 Tutshi) could benefit from snow survey measurements, the others could not. For larger watershed
496 with denser meteorological networks, snow assimilation may prove to be superfluous. Overall,
497 where snow assimilation significantly improves the results, it can be concluded that the
498 corresponding meteorological forcing does not have the expected accuracy for hydrologic
499 modelling purposes, including the assessment of the meteorological network density which is the
500 subject of the next analysis in this study.

501 -- Table 7 here --

502 **4.3 Network sensitivity analysis**

503 The information gained from the validation stage was used to decide whether the assessments
504 should be undertaken with/without the assimilation of snow course data. The proxy validations
505 indicated that at least in Aishihik, CaPA data do not have the required accuracy, while the
506 validations in the other two basins (Mayo and Upper Yukon) were promising. Therefore, in
507 Aishihik, the network assessment was carried out while assimilating the snow course
508 measurements. In Mayo and Upper Yukon, no snow assimilation was performed when evaluating
509 the impact of different network scenarios. Even though any proposed additional station would
510 probably be equipped with various measuring apparatus for different meteorological variables, the
511 network augmentation assessment was carried out with the assumption that the network would be

512 mainly measuring precipitation. This is mainly due to the fact that precipitation demonstrates a lot
513 more spatial variability than other meteorological variables (e.g., temperature, wind).

514 Fig. 7 shows the variation of the NSE, KGE, and absolute PBias scores in Mayo, Aishihik,
515 and Upper Yukon with the changing resolution of the pseudo-network scenarios (for descriptions
516 of the scores, see the supplementary materials). In Mayo (thick lines in all figures), as the network
517 resolution decreases (and so does the network density) from 0.10° to 0.35° , the scores go through
518 two distinct areas of variation. First, decreasing the network resolution from 0.10° to 0.30° results
519 only in marginal drops in all three performance scores. In comparison, the performance of the
520 CaPA precipitation products for a network with a given resolution of 0.30° or higher is better than
521 that of the current meteorological precipitation network (shown by horizontal lines). The
522 fluctuations and the unexpected drops in performance scores in this range are an artifact of the
523 spatial variability of precipitation that has not been fully resolved by certain grid points. This
524 phenomenon which is known as singularity has been reported previously by Abbasnezhadi et al.
525 (2019) and Dong et al. (2005). Decreasing the network density below 0.30° , results in substantial
526 performance deterioration to an extent well below the current sparse MSC network. This indicates
527 that the limit at which the CaPA gridded data can outperform the existing network in Mayo is
528 limited to a network with a density of at least 0.30° .

529 -- Fig. 7 here --

530 The variation of the NSE, KGE, and absolute PBias in Aishihik with changing network
531 resolution are shown by dashed lines and compares the performance of the pseudo-network
532 scenarios constructed based on the CaPA grid definition with the current MSC network in the
533 basin. The same overall trend of variation previously observed in Mayo is evident here too where
534 the scores drop (although less abruptly) after negligible changes before the threshold network

535 density. The less sudden drop is an expected attenuation consequence of a larger drainage area
536 which is more evidently manifested by the NSE scores which is known to be a sensitive parameter
537 to peak discharge values (see Abbasnezhadi et al., 2019 for the same performance outcome). In
538 Aishihik, the network resolution threshold cannot be explicitly inferred. The variation of the NSE
539 indicates that for every decrease in resolution there is a decrease in performance that is rather of
540 the same order of magnitude for all resolutions, whereas those of KGE and PBias assert the 0.4°
541 pseudo-network to entail the optimal resolution below which the accuracy of the ensued flow
542 simulations degrades significantly. Any higher-density network would cause the scores to level
543 off and little would be gained by further increasing the network density. The asserted network
544 density threshold of 0.4° derived for Aishihik resembles the performance established by the current
545 MSC meteorological network in the basin. Moreover, this threshold value is also slightly higher
546 than the one determined for Mayo. This was an anticipated outcome as in basins with a larger
547 drainage area, representativeness errors are averaged out which makes missing a storm event less
548 impactful on the overall network precision. In contrast, in smaller basins (as in Mayo), mesoscale
549 precipitation systems are essentially significant for capturing proper flow statistics. Accordingly,
550 a higher network threshold value can already be anticipated for Upper Yukon which has an even
551 larger drainage area than that of Aishihik.

552 In Upper Yukon (thin lines), the same features previously observed in Mayo and Aishihik are
553 apparent, while a higher network threshold value is resolved. Similar to what was indicated for
554 Aishihik, a network resolution threshold cannot be explicitly inferred in Upper Yukon. Arguably,
555 if Pbias changes are ignored (which asserts the 0.7° pseudo-network to entail the optimal
556 resolution), it can be claimed that the 0.5° pseudo-network would be optimal. A pseudo-network
557 with a density threshold value between 0.5° and 0.7° would as such provide an optimal resolution

558 range. Quite interestingly, the current MSC network maintains an accuracy which is comparable
559 in performance to the highest network density of the original CaPA network.

560 **5. Summary and Conclusions**

561 This study is at the crossroad between meteorological data assimilation (in which precipitation
562 observations are merged into numerically modelled precipitation data), and hydrological data
563 assimilation (in which snow survey data are merged into streamflow forecast). Before applying
564 assimilated precipitation products in meteorological network assessment, first it is required to
565 validate the accuracy of these products. In this study, it is indicated that since assimilation of snow
566 survey data could provide the benchmark for accurate flow estimation, it would then be possible
567 to evaluate the accuracy of precipitation assimilation products through the proxy-validation of
568 precipitation analysis in such a hydrologic system. The HYDROTEL model snow data assimilation
569 (DA) routine is one such example which provides the opportunity to investigate the added value
570 of using the CaPA-RDPA data for application in meteorological network assessment in sparsely
571 gauged Nordic basins.

572 The hydrologic footprint of CaPA-RDPA data and MSC ground observations were validated
573 against hydrometric observations. This validation was performed to examine whether assimilating
574 snow monitoring information in HYDROTEL can offset the adverse effects of precipitation data
575 scarcity in Yukon. When snow assimilation could significantly improve the flow simulation
576 outcomes, it was concluded that the corresponding meteorological forcing (either CaPA-RDPA
577 data or ground observations; in this instance, MSC stations) could not exclusively provide the
578 required accuracy for hydrologic modelling purposes. The proxy validation of the CaPA-RDPA
579 data indicated that the gridded analysis products enjoy the level of accuracy required for accurate
580 flow simulation in Mayo and Upper Yukon which does not entail the application of snow

581 assimilation in HYDROTEL. In Aishihik, however, the validations demonstrated that the regional
582 precipitation analysis does not have the required accuracy, and therefore, assimilation of observed
583 snow course information had a significant impact on the flow estimation accuracy. Based on the
584 results of these experiments, it can be concluded that although these basins are all located within
585 similar ecoclimatic zones in southern Yukon and in the proximity of each other, the distribution
586 of snow course sites and precipitation gauges have left a substantial impact on the accuracy of
587 precipitation and snow assimilation procedures which directly affect the accuracy of flow
588 simulations. These results indicate the importance of the snow assimilation routine in HYDROTEL
589 to embed crucial information not readily available from precipitation forcing data. This approach
590 and the lessons learned may also benefit watersheds in other parts of the world facing similar
591 challenges related to incorporating accurate data when such information is not embedded within
592 the forcing data.

593 With the experiments in hand, a network augmentation assessment was carried out
594 subsequently by incorporating the value of data and products available from the CaPA assimilation
595 system with the assumption that the network would be mainly measuring precipitation. The
596 assessment indicated that a number of additional stations can be installed in each basin to increase
597 the accuracy for streamflow simulation. It is worth reiterating that the analysis was performed
598 based on CaPA-RDPA data and having real measurements on the ground could prove to require
599 fewer stations, especially for Aishihik and Mayo. In addition, the network was assessed in an
600 uncontrolled mode where no observation error was added during the analysis to simulate the
601 impact of such errors (including those related to solid precipitation in winter and convective storms
602 during summer). Instead, CaPA-RDPA data were used directly into the assessment since the
603 assumption of accuracy was validated prior to undertaking the assessment. Given that in the CaPA

604 system, precipitation measurements are subjected to various quality control (QC) procedures
605 before being assimilated, the RDPA products can, therefore, be assumed to be of relatively proper
606 quality. However, the implication of such an assumption is that, the optimal number of stations
607 derived for each basin is valid when those stations satisfy CaPA QC procedures too. In other words,
608 if the quality of measurements available from the proposed extended network can satisfy CaPA
609 QC, they could equally benefit the CaPA system. Moreover, it is ultimately beneficial if any
610 additional precipitation station which can be directly used for flow forecasting in HYDROTEL
611 may also be used for the similar purpose indirectly when embedded into the products of the CaPA
612 assimilation system. Also, if existing snow survey sites could provide the required SWE data for
613 hydrologic snow assimilation, the framework introduced in this study could be easily
614 implemented. Otherwise, in case a network assessment is to be undertaken in a basin where such
615 data are not readily available, proper arrangements should be made to first conduct snow surveys.

616 **Acknowledgements**

617 The authors wish to gratefully acknowledge the financial support from Natural Sciences and
618 Engineering Research Council of Canada (NSERC) and Yukon Energy (YE) through
619 Collaborative (#CRDPJ 499954-16) and Applied (#CARD2 500263-16) Research and
620 Development grants. This project would not have been possible without substantial contributions
621 from staffs at Yukon Research Centre, namely Brian Horton and Maciej Stetkiewicz; at INRS,
622 Sébastien Tremblay; and at YE, Shannon Mallory, Kevin Maxwell, and Andrew Hall. We would
623 like to also acknowledge the following organizations for their readily available online data used in
624 this study: Meteorological Survey of Canada, Water Survey of Canada, Environment and Climate
625 Change Canada, Water Resources Branch at Environment Yukon, Yukon Energy, and Natural
626 Resources Conservation Service at United States Department of Agriculture. The authors declare
627 no conflict of interests in this work.

628 **References**

- 629 Abbasnezhadi, K. 2017. *Influence of meteorological network density on hydrological modeling*
630 *using input from the Canadian Precipitation Analysis (CaPA)*. PhD Thesis, Winnipeg,
631 Manitoba, Canada: University of Manitoba. <http://hdl.handle.net/1993/32177>.
- 632 Abbasnezhadi, K., A. N. Rousseau, K. A. Koenig, Z. Zahmatkesh, and A. M. Wruth. 2019.
633 "Hydrological assessment of meteorological network density through dataassimilation
634 simulation." *Journal of Hydrology* 569: 844-858.
635 doi:<https://doi.org/10.1016/j.jhydrol.2018.12.027>.
- 636 Andreadis, K. M., and D. P. Lettenmaier. 2006. "Assimilating remotely sensed snow
637 observations into a macroscale hydrology model." *Advances in Water Resources* 29: 872-
638 886. doi:<https://doi.org/10.1016/j.advwatres.2005.08.004>.
- 639 Arulampalam, M. S., S. Maskell, N. Gordon, and T. Clapp. 2002. "A tutorial on particle filters
640 for on-line nonlinear/non-Gaussian Bayesian tracking." *IEEE Transactions on Signal*
641 *Processing* 50: 174-188. doi:<https://doi.org/10.1109/78.978374>.
- 642 Asadzadeh, M., and B. Tolson. 2009. "A New Multi- objective Algorithm, Pareto Archived
643 DDS." Edited by G. et al. Raidl. *11th Annual Conference on Genetic and Evolutionary*
644 *Computation Conference (GECCO 2009)*. New York, NY: Association for Computing
645 Machinery. 1963-1966. doi:<https://doi.org/10.1145/1570256.1570259>.
- 646 Asadzadeh, M., and B. Tolson. 2013. "Pareto archived dynamically dimensioned search with
647 hypervolume-based selection for multi-objective optimization." *Engineering Optimization* 45
648 (12): 1489-1509. doi:<https://doi.org/10.1080/0305215X.2012.748046>.
- 649 Barrett, A. P. 2003. *National operational hydrologic remote sensing center snow data*
650 *assimilation system (SNODAS) products at NSIDC*. Special Rep. 11, Boulder, CO, USA:
651 NSIDC, 19. Accessed December 14, 2018.
652 https://nsidc.org/pubs/documents/special/nsidc_special_report_11.pdf.
- 653 Boluwade, A., K.-Y. Zhao, T. Stadnyk, and P. Rasmussen. 2018. "Towards validation of the
654 Canadian Precipitation Analysis (CaPA) for hydrologic modeling applications in the
655 Canadian Prairies." *Journal of Hydrology* 556: 1244-1255.
656 doi:<https://doi.org/10.1016/j.jhydrol.2017.05.059>.
- 657 Boni, G., F. Castelli, S. Gabellani, G. Machiavello, and R. Rudari. 2010. "Assimilation of
658 MODIS snow cover and real time snow depth point data in a snow dynamic model."
659 *Geoscience and Remote Sensing Symposium (Geoscience and Remote Sensing Symposium)*
660 1788-1791. doi:<https://doi.org/10.1109/IGARSS.2010.5648989>.
- 661 Bouda, M., A. N. Rousseau, B. Konan, P. Gagnon, and S. J. Gumiere. 2012. "Bayesian
662 Uncertainty Analysis of the Distributed Hydrological Model HYDROTEL." *Journal of*
663 *Hydrologic Engineering* 17 (9): 1021-1032. doi:[https://doi.org/10.1061/\(ASCE\)HE.1943-5584.0000550](https://doi.org/10.1061/(ASCE)HE.1943-5584.0000550).

- 665 Bouda, M., A. N. Rousseau, S. J. Gumiere, P. Gagnon, B. Konan, and R. Moussa. 2013.
 666 "Implementation of an automatic calibration procedure for HYDROTEL based on prior OAT
 667 sensitivity and complementary identifiability analysis." *Hydrological Processes* 28 (12):
 668 3947-3961. doi:<https://doi.org/10.1002/hyp.9882>.
- 669 Bouda, Médard, Alain N Rousseau, Silvio J Gumiere, Patrick Gagnon, Brou Konan, and Roger
 670 Moussa. 2014. "Implementation of an automatic calibration procedure for HYDROTEL
 671 based on prior OAT sensitivity and complementary identifiability analysis." *Hydrological*
 672 *Processes* 28 (12): 3947-3961. doi:<https://doi.org/10.1002/hyp.9882>.
- 673 Brabets, T. P., and M. A. Walvoord. 2009. "Trends in streamflow in the Yukon River Basin from
 674 1944 to 2005 and the influence of the pacific decadal oscillation." *Journal of Hydrology* 371
 675 (1-4): 108-119. doi:<https://doi.org/10.1016/j.jhydrol.2009.03.018>.
- 676 Brasnett, B. 1999. "A global analysis of snow depth for numerical weather prediction." *Journal*
 677 *of applied meteorology* 38 (6): 726-740. doi:[https://doi.org/10.1175/1520-0450\(1999\)038<0726:AGAOSD>2.0.CO;2](https://doi.org/10.1175/1520-0450(1999)038<0726:AGAOSD>2.0.CO;2).
- 679 Clark, M. P., A. G. Slater, A. P. Barrett, L. E. Hay, G. J. McCabe, B. Rajagopalan, and G. H.
 680 Leavesley. 2006. "Assimilation of snow covered area information into hydrologic and land-
 681 surface models and land-surface models." *Advances in Water Resources* 29: 1209-1221.
 682 doi:<https://doi.org/10.1016/j.advwatres.2005.10.001>.
- 683 De Lannoy, G. J. M., R. H. Reichle, K. R. Arsenault, P. R. Houser, S. Kumar, N. E. C. Verhoest,
 684 and V. R. N. Pauwels. 2012. "Multiscale assimilation of Advanced Microwave Scanning
 685 Radiometer-EOS snow water equivalent and Moderate Resolution Imaging
 686 Spectroradiometer snow cover fraction observations in northern Colorado." *Water Resources*
 687 *Research* 48: W01522. doi:<https://doi.org/10.1029/2011WR010588>.
- 688 Deacu, D., V. Fortin, E. Klyszejko, C. Spence, and P. Blanken. 2012. "Predicting the net basin
 689 supply to the Great Lakes with a hydrometeorological model." *Journal of Hydrometeorology*
 690 13 (6): 1739-1759. doi:<https://doi.org/10.1175/JHM-D-11-0151.1>.
- 691 Dong, X., C. M. Dohmen-Janssen, and M. J. Booij. 2005. "Appropriate spatial sampling of
 692 rainfall or flow simulation." *Hydrological Sciences Journal* 50 (2): 279-298.
 693 doi:<https://doi.org/10.1623/hysj.50.2.279.61801>.
- 694 Drusch, M., D. Vasiljevic, and P. Viterbo. 2004. "ECMWF's global snow analysis: Assessment
 695 and revision based on satellite observations." *Journal of Applied Meteorology* 43: 1282-1294.
 696 doi:[https://doi.org/10.1175/1520-0450\(2004\)043%3C1282:EGSAAA%3E2.0.CO;2](https://doi.org/10.1175/1520-0450(2004)043%3C1282:EGSAAA%3E2.0.CO;2).
- 697 Duan, Q., Gupta, H. V., S. Sorooshian, A. N. Rousseau, and R. Turcotte. 2003. *Advances in*
 698 *calibration of watershed models*. Water Science and Application. Vol. 6. Washigton, D.C.:
 699 American Geophysical Union. doi:<https://doi.org/10.1029/WS006>.
- 700 Durand, M., and S. A. Margulis. 2008. "Effects of uncertainty magnitude and accuracy on
 701 assimilation of multi-scale measurements for snowpack characterization." *Journal of*

- 702 *Geophysical Research Atmosphere* 113 (D2): D02105.
 703 doi:<https://doi.org/10.1029/2007JD008662>.
- 704 Eum, H., D. Yonas, and T. Prowse. 2014. "Uncertainty in modelling the hydrologic responses of
 705 a large watershed: a case study of the Athabasca River basin, Canada." *Hydrological*
 706 *Processes* 28 (14): 4272-4293. doi:<https://doi.org/10.1002/hyp.10230>.
- 707 Evensen, G. 1994. "Sequential data assimilation with a nonlinear quasi-geostrophic model using
 708 Monte Carlo methods to forecast error statistics." *Journal of Geophysical Research* 99:
 709 10143-10162. doi:<https://doi.org/10.1029/94JC00572>.
- 710 Feyen, L., R. Vázquez, K. Christiaens, O. Sels, and J. Feyen. 2000. "Application of a distributed
 711 physically-based hydrological model to a medium size catchment." *Hydrology and Earth*
 712 *System Sciences* 4 (1): 47-63. doi:<https://doi.org/10.5194/hess-4-47-2000>.
- 713 Fortin, J. P., R. Turcotte, S. Massicotte, R. Moussa, J. Fitzback, and J. P. Villeneuve. 2001b. "A
 714 distributed watershed model compatible with remote sensing and GIS data, II: Application to
 715 Chaudière Watershed." *Journal of Hydrologic Engineering* 6 (2): 100-108.
 716 doi:[https://doi.org/10.1061/\(ASCE\)1084-0699\(2001\)6:2\(100\)](https://doi.org/10.1061/(ASCE)1084-0699(2001)6:2(100)).
- 717 Fortin, J. P., R. Turcotte, S. Massicotte, R. Moussa, J. Fitzback, and J. P. Villeneuve. 2001a.
 718 "Distributed watershed model compatible with remote sensing and GIS data, I: Description
 719 of model." *Journal of Hydrological Engineering* 6 (2): 91-99.
 720 doi:[https://doi.org/10.1061/\(ASCE\)1084-0699\(2001\)6:2\(91\)](https://doi.org/10.1061/(ASCE)1084-0699(2001)6:2(91)).
- 721 Fortin, V., G. Roy, N. Donaldson, and A. Mahidjiba. 2015. "Assimilation of radar quantitative
 722 precipitation estimations in the Canadian Precipitation Analysis (CaPA)." *Journal of*
 723 *Hydrology* 531: 296-307. doi:<https://doi.org/10.1016/j.jhydrol.2015.08.003>.
- 724 Foulon, É., and A. N. Rousseau. 2018. "Equifinality and automatic calibration: What is the
 725 impact of hypothesizing an optimal parameter set on modelled hydrological processes?"
 726 *Canadian Water Resources Journal* 43 (1): 47-67.
 727 doi:<https://doi.org/10.1080/07011784.2018.1430620>.
- 728 Foulon, É., M. Blanchette, and A. N. Rousseau. 2019. "Sensitivity and uncertainty analysis of a
 729 semi-distributed model used for the quantitative assessment of watershed-scale hydrological
 730 services of wetlands." *Fall Meeting 2019*. San Francisco, CA: American Geophysical Union.
 731 H53L-1951. <https://ui.adsabs.harvard.edu/abs/2019AGUFM.H53L1951F/abstract>.
- 732 Gbambie, A. B., Poulin A., M. A. Boucher, and R. Arsenault. 2016. "Added value of alternative
 733 information in interpolated precipitation datasets for hydrology." *Journal of*
 734 *Hydrometeorology* 18 (1): 247-264. doi:<https://doi.org/10.1175/JHM-D-16-0032.1>.
- 735 Gelb, A. 1974. "Optimal linear filtering." In *Applied Optimal Estimation*, 102-155. Cambridge,
 736 MA, USA: MIT Press.
- 737 Grünewald, T., and M. Lehning. 2015. "Are flat- field snow depth measurements representative?
 738 A comparison of selected index sites with areal snow depth measurements at the small

- 739 catchment scale." *Hydrological Processes* 29 (7): 1717-1728.
740 doi:<https://doi.org/10.1002/hyp.10295>.
- 741 Gupta, H. V., Kling, H., K. K. Yilmaz, and G. F. Martinez. 2009. "Decomposition of the mean
742 squared error and NSE performance criteria: Implications for improving hydrological
743 modelling." *Journal of Hydrology* 377 (1-2): 80-91.
744 doi:<https://doi.org/10.1016/j.jhydrol.2009.08.003>.
- 745 Haghnegahdar, A., B. A. Tolson, B. Davison, F. R. Seglenieks, E. Klyszejko, and E. D. Soulis.
746 2014. "Calibrating Environment Canada's MESH modelling system over the Great Lakes
747 basin." *Atmosphere-Ocean* 52 (4): 281-293.
748 doi:<https://doi.org/10.1080/07055900.2014.939131>.
- 749 Hanes, C. C., P. Jain, M. Flannigan, and G. Roy. 2016. "Evaluation of the Canadian Precipitation
750 Analysis (CaPA) to improve forest fire danger rating." *International Journal of Wildland
751 Fire* 26 (6): 509-522. doi:<https://doi.org/10.1071/WF16170>.
- 752 Helmert, J., Şorman A. Ş., R. A. Montero, C. De Michele, P. De Rosnay, M. Dumont, D. C.
753 Finger, et al. 2018. "Review of Snow Data Assimilation Methods for Hydrological, Land
754 Surface, Meteorological and Climate Models: Results from a COST HarmoSnow Survey." *Geosciences* 8 (12): 489. doi:<https://doi.org/10.3390/geosciences8120489>.
- 756 Huang, C., A. J. Newman, M. P. Clark, A. W. Wood, and X. Zheng. 2017. "Evaluation of snow
757 data assimilation using the ensemble Kalman filter for seasonal streamflow prediction in the
758 western United States." *Hydrology and Earth System Sciences* 21: 635-650.
759 doi:<https://doi.org/10.5194/hess-21-635-2017>.
- 760 Leisenring, M., and H. Moradkhani. 2011. "Snow water equivalent prediction using Bayesian
761 data assimilation methods." *Stochastic Environmental Research and Risk Assessment* 25:
762 253-270. doi:<https://doi.org/10.1007/s00477-010-0445-5>.
- 763 Li, D., D. P. Lettenmaier, S. A. Margulis, and K. Andreadis. 2019. "The value of accurate high-
764 resolution and spatially continuous snow information to streamflow forecasts." *Journal of
765 Hydrometeorology* 20: 731-749. doi:<https://doi.org/10.1175/JHM-D-18-0210.1>.
- 766 Liston, G. E., R. A., Sr. Pielke, and E. M. Greene. 1999. "Improving first-order snow-related
767 deficiencies in a regional climate model." *Journal of Geophysical Research* 104: 19559-
768 51567. doi:<https://doi.org/10.1029/1999JD900055>.
- 769 Liu, Y., C. D. Peters-Lidard, S. Kumar, J. L. Foster, M. Shaw, Y. Tian, and G. M. Fall. 2013.
770 "Assimilating satellite-based snow depth and snow cover products for improving snow
771 predictions in Alaska." *Advances in Water Resources* 54: 208-227.
772 doi:<https://doi.org/10.1016/j.advwatres.2013.02.005>.
- 773 López-Moreno, J. I., S. R. Fassnacht, J. T. Heath, K. N. Musselman, J. Revuelto, J. Latron, E.
774 Morán-Tejeda, and T. Jonas. 2013. "Small scale spatial variability of snow density and depth
775 over complex alpine terrain: Implications for estimating snow water equivalent." *Advances in
776 Water Resources* 55: 40-52. doi:<https://doi.org/10.1016/j.advwatres.2012.08.010>.

- 777 Magnusson, J., D. Gustafsson, F. Hüsler, and T. Jonas. 2014. "Assimilation of point SWE data
778 into a distributed snow cover model comparing two contrasting methods." *Water Resources*
779 *Research* 50 (10): 7816-7835. doi:<https://doi.org/10.1002/2014WR015302>.
- 780 Mahfouf, J. F., B. Brasnett, and S. Gagnon. 2007. "A Canadian precipitation analysis (CaPA)
781 project: Description and preliminary results." *Atmosphere-Ocean* 45 (1): 1-17.
782 doi:<https://doi.org/10.3137/ao.v450101>.
- 783 Matott, L. S. 2017. "OSTRICH: an Optimization Software Tool." Buffalo, NY: University at
784 Buffalo Center for Computational Research. 79.
785 www.eng.buffalo.edu/~lsmatott/Ostrich/OstrichMain.html.
- 786 Miller, R. N., M. Ghil, and F. Gauthiez. 1994. "Advanced data assimilation in strongly nonlinear
787 dynamical systems." *Journal of the Atmospheric Sciences* 51 (8): 1037-1056.
788 doi:[https://doi.org/10.1175/1520-0469\(1994\)051%3C1037:ADAISN%3E2.0.CO;2](https://doi.org/10.1175/1520-0469(1994)051%3C1037:ADAISN%3E2.0.CO;2).
- 789 Moradkhani, H. 2008. "Hydrologic remote sensing and land surface data assimilation." *Sensors* 8
790 (5): 2986-3004. doi:<https://doi.org/10.3390/s8052986>.
- 791 Nagler, T., H. Rott, P. Malcher, and F. Müller. 2008. "Assimilation of meteorological and remote
792 sensing data for snowmelt runoff forecasting." *Remote Sensing of Environment* 112: 1408-
793 1420. doi:<https://doi.org/10.1016/j.rse.2007.07.006>.
- 794 Noël, P., A. N. Rousseau, C. Paniconi, and D. F. Nadeau. 2014. "An algorithm for delineating
795 and extracting hillslopes and hillslope width functions from gridded elevation data." *Journal*
796 *of Hydrologic Engineering* 19 (2): 366-374. doi:[http://dx.doi.org/10.1061/\(ASCE\)HE.1943-5584.0000783](http://dx.doi.org/10.1061/(ASCE)HE.1943-5584.0000783).
- 798 Piazzzi, G., G. Thirel, L. Campo, and S. Gabellani. 2018. "A particle filter scheme for
799 multivariate data assimilation into a point-scale snowpack model in an Alpine environment."
800 *Cryosphere* 12 (7): 2287-2306. doi:<https://doi.org/10.5194/tc-12-2287-2018>.
- 801 Pierre, A., S. Jutras, S. Craig, J. Kochendorfer, V. Fortin, and F. Anctil. 2019. "Evaluation of
802 Catch Efficiency Transfer Functions for Unshielded and Single-Alter-Shielded Solid
803 Precipitation Measurements." *Journal of Atmospheric and Oceanic Technology* 36 (5): 865-
804 881. doi:<https://doi.org/10.1175/JTECH-D-18-0112.1>.
- 805 Razavi, S., R. Sheikholeslami, H. V. Gupta, and A. Haghnegahdar. 2019. "VARS-TOOL: A
806 toolbox for comprehensive, efficient, and robust sensitivity and uncertainty analysis."
807 *Environmental Modelling & Software* 112: 95-107.
808 doi:<https://doi.org/10.1016/j.envsoft.2018.10.005>.
- 809 Rousseau, A. N., J.-P. Fortin, R. Turcotte, A. Royer, S. Savary, F. Quévy, P. Noël, and C.
810 Paniconi. 2011. "PHYSITEL, a specialized GIS for supporting the implementation of
811 distributed hydrological models." *Water News-Official Magazine of the Canadian Water*
812 *Resources Association* 31 (1): 18-20.

- 813 Saloranta, T. M. 2016. "Operational snow mapping with simplified data assimilation using the
814 seNorge snow model." *Journal of Hydrology* 538: 314-325.
815 doi:<https://doi.org/10.1016/j.jhydrol.2016.03.061>.
- 816 Samuel, J., A. N. Rousseau, K. Abbasnezhadi, and S. Savary. 2019. "Development and
817 evaluation of a hydrologic data-assimilation scheme for short-range flow and inflow
818 forecasts in a data-sparse high-latitude region using a distributed model and ensemble
819 Kalman filtering." *Advances in Water Resources* 130: 198-220.
820 doi:<https://doi.org/10.1016/j.advwatres.2019.06.004>.
- 821 Slater, A. G., and M. P. Clark. 2006. "Snow data assimilation via an ensemble Kalman filter."
822 *Journal of Hydrometeorology* 7: 478-493. doi:<https://doi.org/10.1175/JHM505.1>.
- 823 Strong, W. L. 2013. "Ecoclimatic Zonation of Yukon (Canada) and Ecoclinal Variation in
824 Vegetation." *Arctic* 66 (1): 52-67. doi:<https://doi.org/10.14430/arctic4266>.
- 825 Su, H., Z. L. Yang, G. Y. Niu, and R. E. Dickinson. 2008. "Enhancing the estimation of
826 continental-scale snow water equivalent by assimilating MODIS snow cover with the
827 ensemble Kalman filter." *Journal of Geophysical Research Atmospheres* 113 (D8): D08120.
828 doi:<https://doi.org/10.1029/2007JD009232>.
- 829 Tolson, B. A., and C. A. Shoemaker. 2007. "Dynamically Dimensioned Search Algorithm for
830 Computationally Efficient Watershed Model Calibration." *Water Resources Research* (Water
831 Resources Research) 43 (1). doi:<https://doi.org/10.1029/2005WR004723>.
- 832 Turcotte, R., A. N. Rousseau, J.-P. Fortin, and J.-P. Villeneuve. 2003. "A process-oriented,
833 multiple-objective calibration strategy accounting for model structure." In *Advances in
834 calibration of watershed models*, edited by Q. Duan, H. V. Gupta, S. Sorooshian, A. N.
835 Rousseau and R. Turcotte, 153-163. Washington, D.C.: American Geophysical Union.
836 doi:<https://doi.org/10.1029/WS006p0153>.
- 837 Turcotte, R., J.-P. Fortin, A. N. Rousseau, S. Massicotte, and J.-P. Villeneuve. 2001.
838 "Determination of the drainage structure of a watershed using a digital elevation model and a
839 digital river and lake network." *Journal of Hydrology* 240 (3-4): 225-242.
840 doi:[https://doi.org/10.1016/S0022-1694\(00\)00342-5](https://doi.org/10.1016/S0022-1694(00)00342-5).
- 841 Turcotte, R., L. G. Fortin, V. Fortin, J.-P. Fortin, and J.-P. Villeneuve. 2007. "Operational
842 analysis of the spatial distribution and the temporal evolution of the snowpack water
843 equivalent in southern Québec, Canada." *Nordic Hydrology* 38 (3): 211-234.
844 doi:<https://doi.org/10.2166/nh.2007.009>.
- 845 Turcotte, R., T.-C. F. Filion, P. Lacombe, V. Fortin, A. Roy, and A. Royer. 2010. "Simulation
846 hydrologique des derniers jours de la crue de printemps: le problème de la neige manquante."
847 *Hydrological Sciences Journal* 55 (6): 872-882.
848 doi:<http://dx.doi.org/10.1080/02626667.2010.503933>.

849 Winstral, A., and D. Marks. 2014. "Long- term snow distribution observations in a mountain
850 catchment: Assessing variability, time stability, and the representativeness of an index site."
851 *Water Resources Research* 50: 293-305. doi:<https://doi.org/10.1002/2012WR013038>.

852 Wong, J. S., S. Razavi, B. R. Bonsal, H. S. Wheeler, and Z. E. Asong. 2017. "Inter-comparison
853 of daily precipitation products for large-scale hydro-climatic applications over Canada."
854 *Hydrology and Earth System Sciences* 21 (4): 2163-2185. doi:[https://doi.org/10.5194/hess-](https://doi.org/10.5194/hess-21-2163-2017)
855 21-2163-2017.

856 Xu, X., S. K. Frey, A. Boluwade, A. R. Erler, O. Khader, D. R. Lapen, and E. Sudicky. 2019.
857 "Evaluation of variability among different precipitation products in the Northern Great
858 Plains." *Journal of Hydrology: Regional Studies* 24: 100608.
859 doi:<https://doi.org/10.1016/j.ejrh.2019.100608>.

860 Zhao, K.-Y. 2013. *Validation of the Canadian Precipitation Analysis (CaPA) for hydrological*
861 *modelling in the Canadian Prairies*. Master's thesis, Winnipeg, Manitoba: University of
862 Manitoba.

863

864

865 Table 1. MSC* meteorological networks in Mayo, Aishihik, and Upper Yukon (see Fig. 2).

Basin	Station Name	Station No.	Period	Time Step	Type
Mayo	ELSA	2100500	1948-1989	Daily	Manual
	Mayo A	2100700	1924-2013	Hourly & Daily	Auto
	Mayo A	2100701	2013-Present	Hourly & Daily	Auto
	Steward Crossing	2101030	1953-2008	Daily	Manual
	MAYOMET	MAYOMET	2018-Present	Hourly & Daily	Auto
Aishihik	Aishihik A	2100100	1943-1966	Hourly & Daily	Manual
	Blanchard River	2100163	1986-2012	Daily	Auto
	Burwash A	2100181	2011-Present	Hourly & Daily	Auto
	Burwash A	2100182	1966-2015	Hourly & Daily	Auto
	Burwash Airport BC	2100184	2013-Present	Hourly & Daily	Auto
	Carmacks CS	2100301	1999-Present	Hourly & Daily	Auto
	Haines Junction	2100630	1944-Present	Hourly & Daily	Auto
	Pelly Ranch	2100880	1898-2015	Daily	Manual
	Takhini River Ranch	2101095	1980-2015	Daily	Manual
	Otter Falls NCP	2100840	1980-2015	Daily	Manual
AISHMET	AISHMET	2018-Present	Hourly & Daily	Auto	
Upper Yukon	Atlin	1200560	1899-Present	Daily	Manual
	Teslin	2101102	1944-Present	Hourly & Daily	Auto
	Whitehorse A	2101303	2012-Present	Hourly & Daily	Auto
	Whitehorse Auto	2101310	2009-Present	Hourly & Daily	Auto
	Fantail Lower	FANTLOW	2012-Present	Hourly	Auto
	Fantail Upper	FANTUPP	2012-Present	Hourly	Auto
	Llewellyn Lower	LLEWLOW	2013-Present	Hourly	Auto
	Llewellyn Upper	LLEWUPP	2013-2016	Hourly	Auto
	Wheaton	WHEATON	2014-Present	Hourly	Auto

866 * MSC: Meteorological Survey of Canada

867 Table 2. WSC* and YE* hydrometric networks in Mayo, Aishihik, and Upper Yukon basins. The
 868 gauges used for the HYDROTEL model calibration are in bold (see Fig. 2).

Basin	Station Name	Station No.	Period	Type
Mayo	Mayo Lake near the Outlet	09DC005	1979-Present	Water Level
	Mayo Lake at the Outlet	YECMAYO	1979-Present	Flow
	Inflow to Mayo Lake (reconstructed)	##0000003	1979-Present	Flow
Aishihik	Aishihik Lake near Whitehorse	08AA005	1972-Present	Water Level
	Sekulmun River at Outlet of Sekulmun Lake	08AA008	1981-Present	Flow & Water level
	Giltana Creek near The Mouth	08AA009	1980-Present	Flow & Water level
	Aishihik River below Aishihik Lake	08AA010	1980-Present	Flow & Water level
	Aishihik Lake near Aishihik	08AA012	1995-2015	Water Level
	Inflow to Aishihik Lake (reconstructed)	#0000003	1980-Present	Flow
Upper Yukon	Atlin River near Atlin	09AA006	1950-Present	Flow
	Wheaton River near Wheaton	09AA012	1955-Present	Flow
	Tutshi River near outlet of Tutshi Lake	09AA013	1956-Present	Flow
	Yukon River at Whitehorse	09AB001	1902-Present	Flow

869 * WSC: Water Survey of Canada; YE: Yukon Energy

870 Table 3. WRB and YE snow course and GMON networks in Mayo, Aishihik, and Upper Yukon

871 (see Fig. 2).

Basin	Station Name	Station No.	Period	Type	Sources*
Mayo	Calumet	09DD-SC01	1975-Present	Depth/SWE	WRB
	Edwards Lake	09DD-SC02	1987-Present	Depth/SWE	WRB
	Mayo Airport A	09DC-SC01A	1968-Present	Depth/SWE	WRB
	Mayo Airport B	09DC-SC01B	1987-Present	Depth/SWE	WRB
	MAYOMET	MAYOMET	2017-Present	GMON	YE
Aishihik	Canyon Lake	08AA-SC01	1975-Present	Depth/SWE	WRB
	Macintosh	09CA-SC02	1976-Present	Depth/SWE	WRB
	Aishihik Lake	08AA-SC03	1944-Present	Depth/SWE	WRB
	AISHMET	AISHMET	2017-Present	GMON	YE
Upper Yukon	Tagish	09AA-SC1	2006-Present	Depth/SWE	WRB
	Montana Mountain	09AA-SC2	2006-Present	Depth/SWE	WRB
	Log Cabin (BC)	09AA-SC3	2006-Present	Depth/SWE	WRB
	Atlin (BC)	09AA-SC4	2006-Present	Depth/SWE	WRB
	Mt. McIntyre	09AB-SC1B	2006-Present	Depth/SWE	WRB
	Whitehorse Airport	09AB-SC2	2006-Present	Depth/SWE	WRB
	Meadow Creek	09AD-SC1	2006-Present	Depth/SWE	WRB
	Moore Creek Bridge (AL)	0034K02	2006-Present	Depth/SWE	USDA-NRCS
	Eaglecrest (AL)	0034J03	2006-Present	Depth/SWE	USDA-NRCS
	Fantail Lower	FANTLOW	2012-2017	GMON	YE
	Fantail Upper	FANTUPP	2012-2017	GMON	YE
	Llewellyn Lower	LLEWLOW	2013-Present	GMON	YE
	Llewellyn Upper	LLEWUPP	2013-2016	GMON	YE
Wheaton	WHEATON	2014-Present	GMON	YE	

* WRB: Water Resources Branch, Environment Yukon; YE: Yukon Energy; USDA-NRCS: United States Department of Agriculture, Natural Resources Conservation Service

872

873 Table 4. HYDROTEL parameter sets associated with each hydrological process. Importance
 874 Level-0 parameters refer to those often physically-based constant (non-calibrated parameters),
 875 while levels 2 and 3 indicate lower importance levels and were not calibrated. Parameters
 876 calibrated in OSTRICH are identified by the importance level of 1. The lower and upper bounds
 877 shown in the table are used in parameter optimization.

Process/Parameter	Unit	Lower Bound	Upper Bound	Importance Level	OSTRICH Code
Vertical water budget: BV3C					
Thickness of the first soil layer	m	0.05	0.60	1	Z1
Thickness of the second soil layer	m	0.05	0.60	1	Z2
Thickness of the third soil layer	m	0.05	0.80	1	Z3
Initial humidity of the first soil layer	--	0.90	0.90	0	--
Initial humidity of the second soil layer	--	0.90	0.90	0	--
Initial humidity of the third soil layer	--	0.90	0.90	0	--
Extinctive coefficient	--	0.3	0.9	2	--
Recession coefficient	m/h	0.0000001	0.00001	1	CR
Drying coefficient	--	0.5	1.0	2	--
Maximal variation of relative humidity of soil layer	--	0.2	0.4	2	--
Interpolation of meteorological variables: Weighted mean of nearest three stations					
Temperature gradient	°C/100 m	-1.5	0.0	1	GT
Precipitation gradient	mm/100 m	0.0	1.5	1	GP
Phase change temperature threshold	°C	-3.5	3.5	1	PPN
Snow accumulation and melt: Mixed degree-day energy budget approach					
Melting rate (soil/snow)	mm/day	0.5	0.5	0	--
Maximal snow density	Kg/m ³	466	466	0	--
Compaction constant	--	0.01	0.01	0	--
Evergreen forest melting temperature threshold	°C	-3.5	3.5	1	SFC
Deciduous forest melting temperature threshold	°C	-3.5	3.5	1	SFF
Open area melting temperature threshold	°C	-3.5	3.5	1	SFD
Evergreen forest melting rate	mm/day °C	1	20	1	TFC
Deciduous forest melting rate	mm/day °C	1	20	1	TFF
Open area melting rate	mm/day °C	1	20	1	TFD
Albedo threshold	--	1	1	0	--
Glacier melt: Mixed degree-day energy-budget approach					
Melting rate	mm/day	1	20	1	MR
Melting temperature threshold	°C	-3.5	3.5	1	TT
Soil temperature and soil frost: Rankinen					
Soil freezing temperature threshold	°C	-1	1	3	--
Potential evapotranspiration: Penman-Monteith					
Standard height for wind measurement	m	2	2	0	--
Standard height for humidity measurement	m	2	2	0	--
Wind speed at the Z elevation	m/s	2	2	0	--
Surface reference vegetation height	m	0.12	0.12	0	--
Stomatal resistance for reference surface	s/m	80	120	2	--
Multiplicative coefficient	--	0.25	1.30	1	FETP
Flow on sub-watersheds towards river network: Kinematic wave					
Manning coefficient for forest land cover classes	--	0.15	0.3	3	--
Manning coefficient for water land cover classes	--	0.015	0.03	3	--
Manning coefficient for other land cover classes	--	0.04	0.1	3	--
Channel flow: Kinematic wave					
Roughness optimization	--	1	1	0	--
Stream width optimization	--	1	1	0	--

878

879 Table 5. Application of snow assimilation during the experiments. × : snow assimilation was
 880 performed during the calibration/stand-alone run, ✓ : snow assimilation was not performed
 881 during the calibration/stand-alone run.

Exp.		Meteorological Forcing	Snow Assimilation ✓ : active / × : inactive	
Set	Run		Calibration	Stand-alone Run
1	1.1	CaPA-RDPA	✓	✓
	1.2		✓	×
2	2.1	MSC Meteorology	✓	✓
	2.2		✓	×

882

883 Table 6. Sampling grid of pseudo-network scenarios (Θ^ν) of different resolutions in decimal arc-
 884 degrees (ν) for each study basin, extracted from the CaPA grid. See individual scenarios in the
 885 supplementary material.

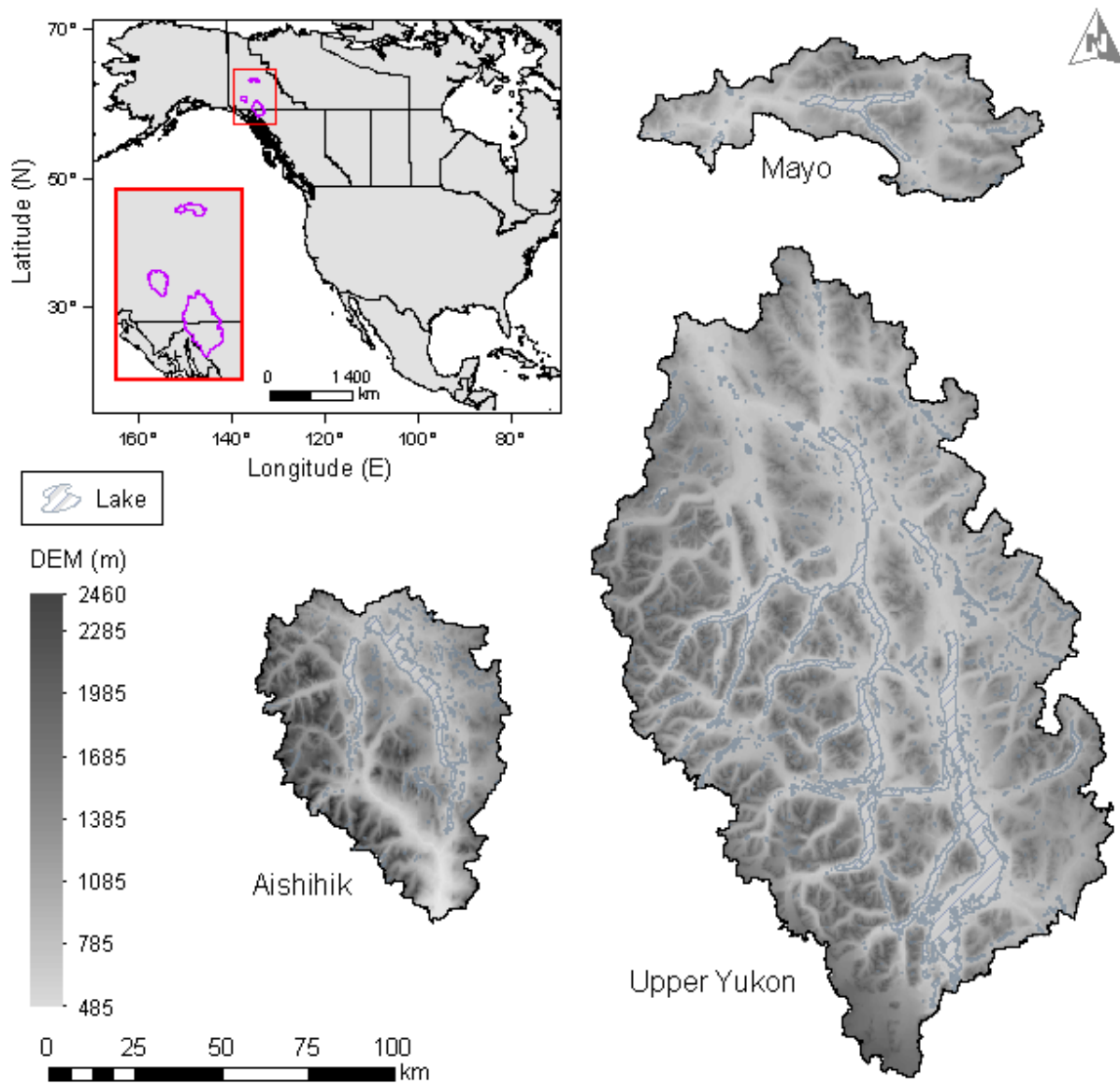
Basin	Sampling grid scenarios
Mayo	$\Theta^\nu \mid \nu \in [0.10^\circ, 0.15^\circ, 0.20^\circ, 0.30^\circ, 0.35^\circ]$
Aishihik	$\Theta^\nu \mid \nu \in [0.10^\circ, 0.20^\circ, 0.30^\circ, 0.40^\circ, 0.50^\circ]$
Upper Yukon	$\Theta^\nu \mid \nu \in [0.10^\circ, 0.20^\circ, 0.30^\circ, 0.40^\circ, 0.50^\circ, 0.60^\circ, 0.70^\circ, 0.80^\circ]$

886

887 Table 7. Significance of the snow assimilation routine in HYDROTEL given the meteorological
 888 forcing for each study basin. Basin denominations are in bold, sub-basins are not. ✓ indicates that
 889 performing snow assimilation for the selected basin has a significant impact, while × shows a
 890 nonsignificant outcome.

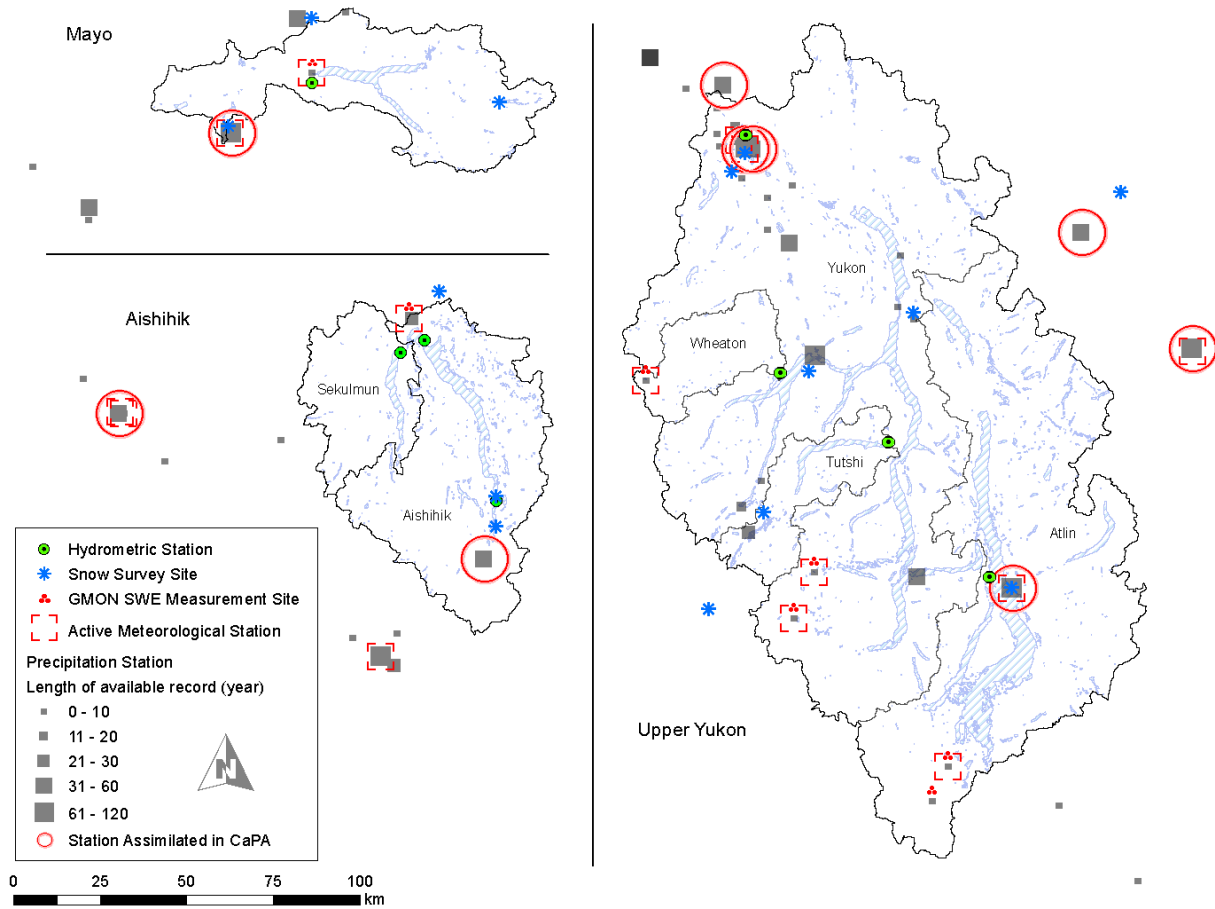
Basin	CaPA-RDPA	MSC meteorology
Mayo	×	✓
Aishihik	✓	×
Sekulmun	✓	×
Upper		
Yukon	×	×
Atlin	×	×
Tutshi	×	✓
Wheaton	✓	×

891



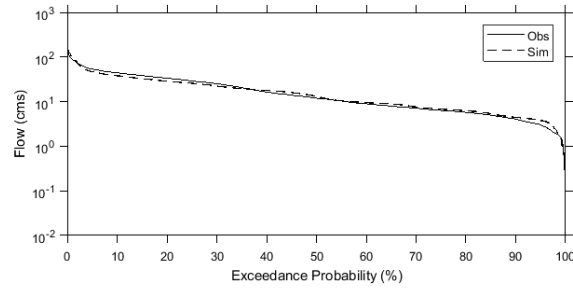
892

893 Fig. 1. The location of Mayo, Aishihik, and Upper Yukon River basins in central and southern
 894 Yukon. The southern half of the Upper Yukon basin is located within northern British Columbia.

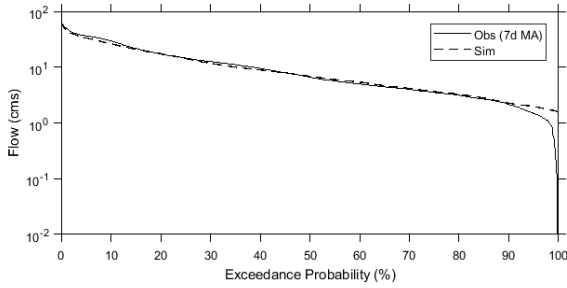


895

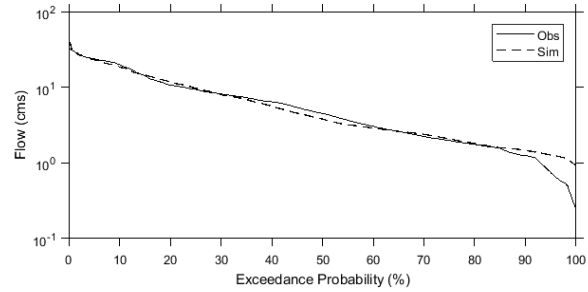
896 Fig. 2. The distribution of meteorological (solid black squares), hydrometric (co-centric green
 897 circles), snow course sites (blue asterisks), and GMON stations (solid red three-dot triangles)
 898 within and in the vicinity of the study basins (Mayo, Aishihik, and Upper Yukon). Meteorological
 899 stations are graduated based on the number of years of available record. Active meteorological
 900 stations (hollow red squares with dashed perimeter) and the synoptic weather stations currently
 901 assimilated in CaPA (hollow red circles) are identified.



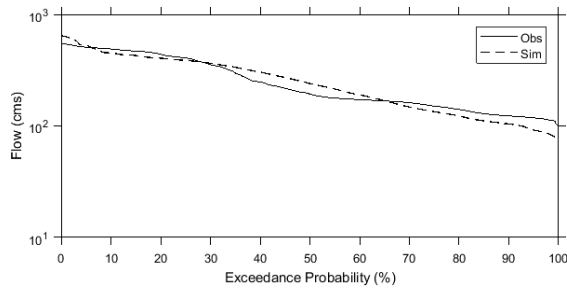
(a) Mayo (##0000003)



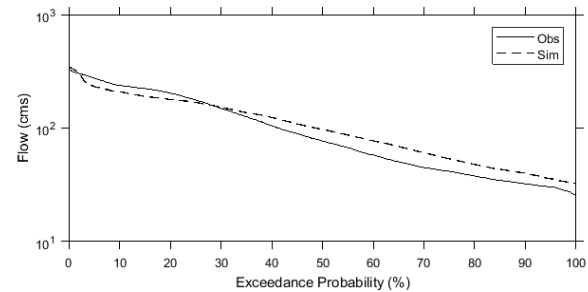
(b) Aishihik (#0000003)



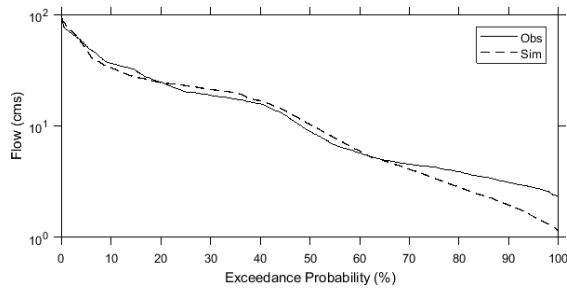
(c) Sekulmun (08AA008)



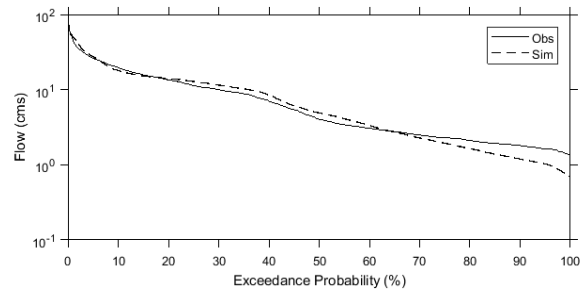
(d) Yukon (09AB001)



(e) Atlin (09AA006)

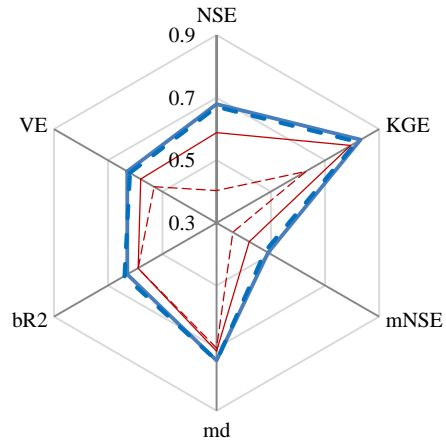


(f) Tutshi (09AA013)



(g) Wheaton (09AA012)

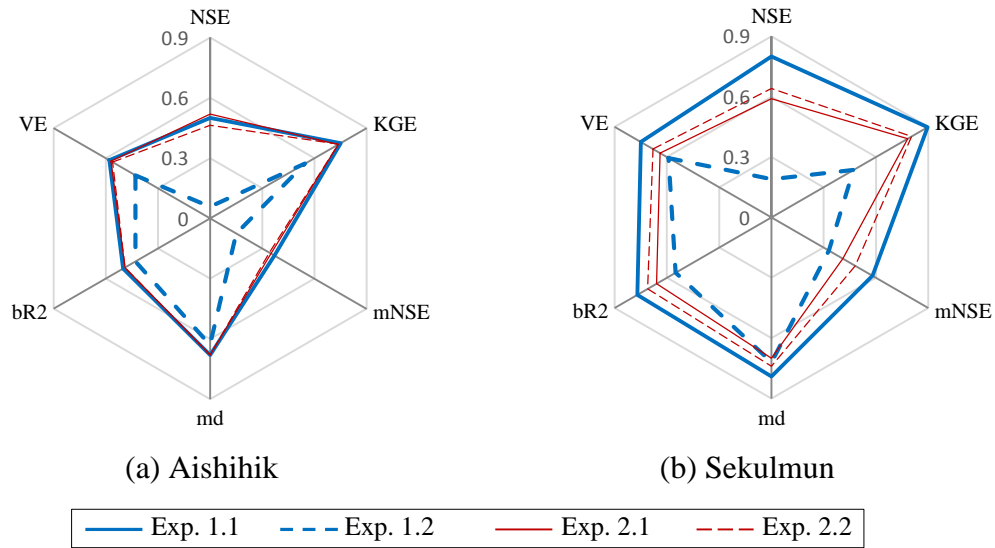
902 Fig. 3. Calibration flow duration curves for different hydrometric stations. Observations are shown
 903 as solid lines and simulations are dashed (refer to the supplementary materials provided in the
 904 online version of this paper to see flow hydrographs).



905



906 Fig. 4. Radial diagram for the performance of the model in response to the set of experiments
 907 completed in Mayo (Station ##0000003). NSE, VE, bR2, md, mNSE, and KGE stand for Nash-
 908 Sutcliffe Efficiency, Volumetric Efficiency, Modified Coefficient of Determination, Modified
 909 Index of Agreement Modified Nash-Sutcliffe Efficiency, and Kling-Gupta Efficiency,
 910 respectively.



911

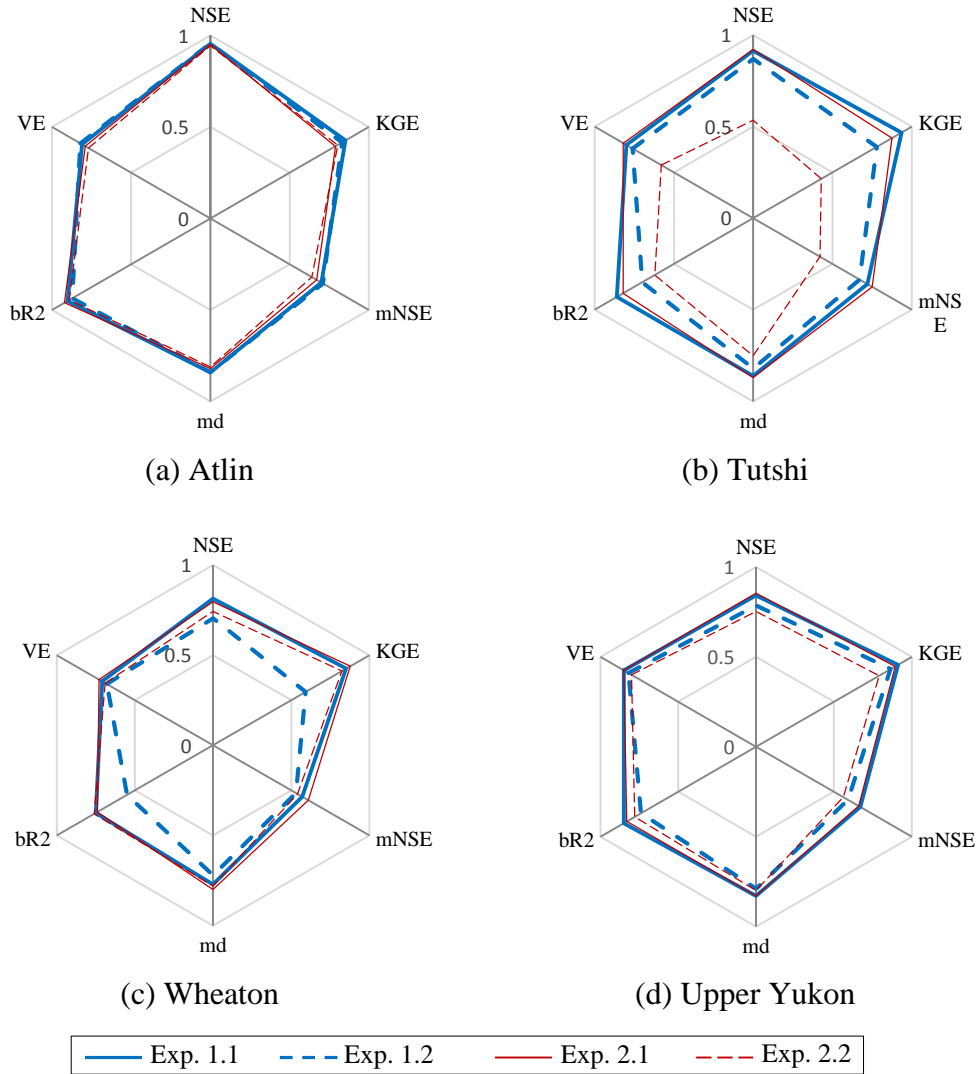
912 Fig. 5. Radial diagrams for the performance of the model in response to the set of experiments

913 completed in Aishihik at (a) Aishihk (Station #0000003), and (b) Sekulmun (Station 08AA008).

914 NSE, VE, bR2, md, mNSE, and KGE stand for Nash-Sutcliffe Efficiency, Volumetric Efficiency,

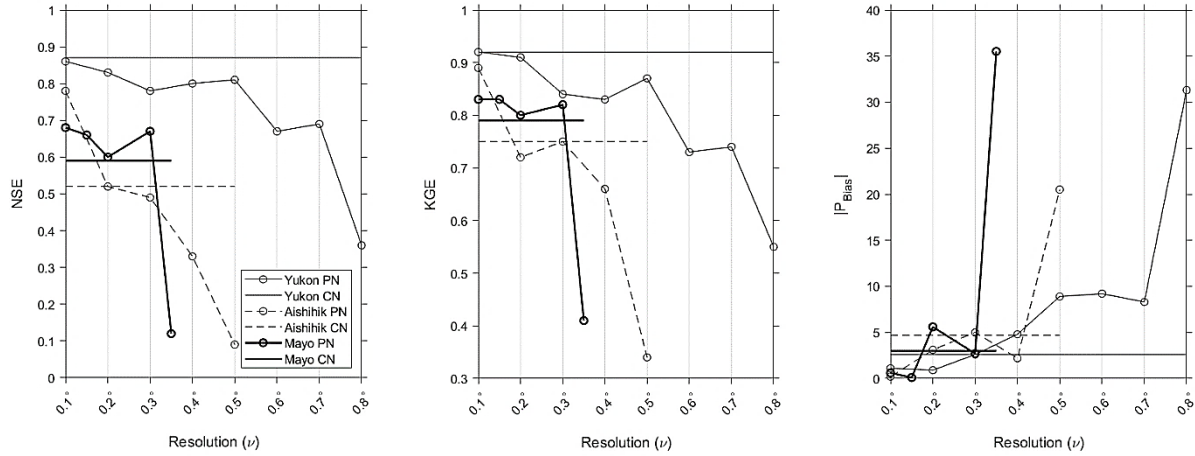
915 Modified Coefficient of Determination, Modified Index of Agreement Modified Nash-Sutcliffe

916 Efficiency, and Kling-Gupta Efficiency, respectively.



917

918 Fig. 6. Radial diagrams for the performance of the model in response to the set of experiments
 919 completed in Upper Yukon at (a) Yukon (Station 09AB001), (b) Tutshi (Station 09AA013),
 920 (c) Wheaton (Station 09AA012), and (d) Atlin (Station 09AA006). NSE, VE, bR2, md, mNSE,
 921 and KGE stand for Nash-Sutcliffe Efficiency, Volumetric Efficiency, Modified Coefficient of
 922 Determination, Modified Index of Agreement Modified Nash-Sutcliffe Efficiency, and Kling-
 923 Gupta Efficiency, respectively.



924 Fig. 7. Variation of the NSE (left), KGE (middle), and absolute PBias (right) in Mayo (thick lines),
 925 Aishihik (dashed lines), and Upper Yukon (thin lines) based on pseudo-networks (PN) resolution
 926 defined in Table 6. The revenue of the current network (CN) in each basin is also shown (horizontal
 927 lines).